Wen, L. *et al.* (2018). *Géotechnique* **68**, No. 9, 749–771 [https://doi.org/10.1680/jgeot.17.P.095]

REVIEW ARTICLE

A statistical review of the behaviour of concrete-face rockfill dams based on case histories

L. WEN*, J. CHAI*†, Z. XU*, Y. QIN* and Y. LI*

The concrete-face rockfill dam (CFRD) has become a preferred dam type, but its design remains largely based on past experiences. Understanding the behaviour of CFRDs is critical to the design and safety assessments of these dams. The main objective of this study is to review the behaviour of CFRDs from the perspective of statistical analysis. A set of monitoring records and construction details of 87 case histories of in-service CFRDs constructed in the past 50 years is collected. The analysed data that are presented are based on a review of the literature. Detailed statistical analyses of post-construction crest settlement and face slab behaviour, settlement of the dam body during construction and leakage after reservoir filling are conducted on the basis of the above-mentioned case histories. Several suggested empirical relationships are obtained by regression analysis to estimate the deformation and seepage behaviour of CFRDs. Findings offer reliable insights into dam behaviour and provide an engineering analogy and reference for the planning, design and construction of CFRDs in the future. The statistical analyses also attempt to identify quantitatively the major influencing factors of the deformation of CFRDs, such as intact rockfill strength, foundation characteristics, valley shape and seepage flow. Intact rockfill strength and foundation characteristics are found to be the main influencing factors of dam deformation behaviour. The results from the statistical analysis of the case histories and the analyses performed are also presented herein.

KEYWORDS: dams; deformation; seepage; settlement; statistical analysis; stress analysis

INTRODUCTION

The concrete-face rockfill dam (CFRD) has become a preferred dam type over the last 50 years since the adoption of the vibratory roller compaction technique (Cooke, 1984; Kan & Taiebat, 2016). Owing to their advantages, numerous CFRDs have been constructed worldwide; some of them are even situated where site conditions are complex, such as the Alto Anchicaya Dam built on a deep alluvium foundation and the Zipingpu Dam built in a strongly seismic zone. CFRDs are currently being developed from a 200 m high level to a 300 m high level. Complex site conditions and large dam height can lead to poor performance, such as large settlements, severe cracking and excessive leakage (Xu *et al.*, 2015). Thus, understanding the behaviour of CFRDs is critical to the design and safety assessments of these dams.

Numerous techniques, including numerical methods, centrifuge model testing and empirical predictive methods, have been developed to evaluate CFRD behaviour properly. Many investigators have performed numerical analyses on CFRD behaviour (Su *et al.*, 2012; Zheng *et al.*, 2013; Jia & Chi, 2015). Some advanced constitutive models (Charles, 2008; Silvani *et al.*, 2009; Karstunen & Yin, 2010; Dolezalova & Hladik, 2011; Elia *et al.*, 2011; Ma *et al.*, 2015; Xiao *et al.*, 2015) and contact analysis methods (Zhang *et al.*, 2004; Qian *et al.*, 2013) have been proposed to characterise dam behaviour. However, the accuracy of numerical analysis results depends mainly on the suitability of the constitutive model of rockfill material and the proper calculation parameters, and the validity of the numerical results requires calibration by in situ measurements. Centrifuge model tests have been performed on CFRDs modelled under complex loading conditions (Xu *et al.*, 2006; Seo *et al.*, 2009). Test results can provide practical insights into dam behaviour, but high cost and experimental limitations hinder the application of such tests to a certain extent. Although CFRDs have become increasingly popular worldwide in recent decades, their design and construction still largely depend on empirical methods and past experiences. Engineering analogy based on case studies obtains responses in line with the reality and is preferable when using a database of numerous well-documented case histories for analysis.

Reliance on the historical performance of existing dams is necessary to estimate dam properties. Clements (1984), Cooke (1984) and Sherard & Cooke (1987) systematically summarised the behaviour of early period CFRDs on the basis of measurements on existing dams, and they proposed empirical methods for estimating crest settlement and face slab deflection. Pinto & Marques (1998), Hunter (2003) and Won & Kim (2008) performed statistical analyses of crest settlement and face slab deflection on the basis of a small number of case histories. Li (2011) systematically summarised the characteristics of a CFRD with a height of more than 129 m in China. Other studies have also used a database that comprises information from various CFRDs to assess dam behaviour (Jiang & Cao, 1993; Kim & Kim, 2008; Seo *et al.*, 2009; Kim *et al.*, 2014). However, the existing databases of case histories are small (no more than 30 cases). In addition, these studies have often concentrated on only one or two deformation behaviours (e.g. crest settlement and face deflection) and on the influencing factors of dam behaviour.

This study collects case history behaviour and conducts a sound statistical review. Data on monitoring records,

Manuscript received 9 April 2017; revised manuscript accepted 10 November 2017. Published online ahead of print 2 January 2018. Discussion on this paper closes on 1 February 2019, for further details see p. ii.

* State Key Laboratory Base of Eco-hydraulic Engineering in Arid Area, Xi'an University of Technology, Xi'an, P. R. China.
† School of Civil Engineering, Xijing University, Xi'an, P. R. China.

Downloaded by [UNIV OF ILLINOIS] on [05/02/20]. Copyright © ICE Publishing, all rights reserved.

construction details and construction materials are gathered for 87 in-service CFRDs. The presented analysed data are based on a review of the literature. The main objective of this study is to review the behaviour of CFRDs from the perspective of statistical analysis. Detailed analyses for post-construction crest settlement and face slab behaviour, settlement of the dam body during construction and leakage after reservoir filling are conducted. The cause and mechanism of a few critical problems (e.g. separation and cracking of the face slab) are discussed. This study also pays close attention to the effect of various factors, including intact rockfill strength, foundation characteristics, valley shape and seepage flow, on dam behaviour.

CURRENT CFRD PRACTICE AND CASE HISTORY DATABASE

Current CFRD practice

The modern practice in CFRD design was described by Cooke (1984). A typical CFRD zoning is shown in Fig. 1. The dam body is usually divided into different zones depending on material type, particle size and purpose. Zones 1A and 1B usually consist of silt or fine sand to seal cracks or joint openings. Zones 2A and 3A consist of processed granular materials that support the face slab. Zones 3B and 3C are the main rockfills composed of large rocks. Medium hard rock or hard rock with unconfined compressive strength (UCS) of 40–80 MPa is the most applicable dam construction material. Soft rock with UCS of less than 30 MPa is also an optional construction material, but it is generally used at a location subjected to small deformation or stress. Natural sands and gravels are good dam construction materials because of their large deformation modulus after compaction. Hunter (2003) classified rockfill as very high (VH) strength with UCS of 70–240 MPa, medium high (MH) strength with UCS of 20–70 MPa and medium (M) strength with UCS of 6–20 MPa. A low-cement extruded curb installed on the cushion layer has been widely used in recently constructed CFRDs (Zhang & Zhang, 2011) to aid in avoiding segregation.

A CFRD usually requires a reasonably good rock foundation. As construction methods evolve and energy demands soar, many dams are being constructed on a compressible alluvium foundation (Fig. 1). Alluvium is composed mainly of gravel, crushed rock and fine sand and is characterised by looseness, lithological discontinuance and uniform or discontinuous particle size distribution (Hanna *et al.*, 1986). A cut-off wall is usually constructed in the alluvium foundation to control seepage and potential erosion (Song & Cui, 2015). Most previous analyses have focused on dams built on a rock foundation. Nevertheless, studies on the behaviour of CFRDs built on alluvium are scarce owing to limited and incomplete data records (Wang & Liu, 2005; Xu *et al.*, 2006; Gan *et al.*, 2014; Wen *et al.*, 2015, 2017). Extensive studies are thus necessary to evaluate and understand dam behaviour and thereby fully utilise river gravels as a dam foundation.

The construction parameters of CFRDs are determined mainly by rockfill quality and type and particle size distribution. Depending on rockfill strength, layer thickness is generally 0·9–2·0 m for the main rockfill. The accepted practice is four passes to eight passes of a minimum 10 t vibrating roller, with a variation in the number of passes, water content and layer thickness (Cooke & Sherard, 1987). Xing *et al.* (2006) conducted placement tests of weak rocks in three CFRDs and found that weak rocks with a layer thickness of 0·8–1·0 m exhibit high density and low porosity after six to eight passes of a 13·5–17 t vibrating roller. They also demonstrated that proper water content is useful for compaction. The proper water content can also reduce post-construction wetting deformation (Mahinroosta *et al.*, 2015).

A rockfill modulus estimation is essential for dam deformation analysis and rockfill selection. Fitzpatrick *et al.* (1985) defined two moduli of deformation for rockfill: the vertical modulus of deformation (E_v), defined from the vertical settlement of rockfill during construction, and the transverse modulus of deformation (E_t), defined from the normal displacement to the upstream face during reservoir filling. These moduli are expressed as

$$E_v = \gamma D H_i / s \tag{1}$$

$$E_t = \gamma_w d h_i / \delta_s \tag{2}$$

where γ is the unit weight of rockfill; γ_w is the unit weight of water; s is the settlement of layer of thickness D owing to dam construction to a thickness H_i above that layer; δ_s is the face slab deflection at depth h_i from the reservoir surface; and d is the height of inclined column normal to face slab. The relevant variables are illustrated in Fig. 1. E_t is an artificial modulus and is only used to estimate face slab deformation. E_v depends on void ratio and rock quality but ignores the effect of valley shape. Numerous proposed empirical approaches are associated with E_v or E_t. For example, Hunter & Fell (2003) and Kim & Kim (2008) proposed empirical relations with E_v to estimate dam body settlement and

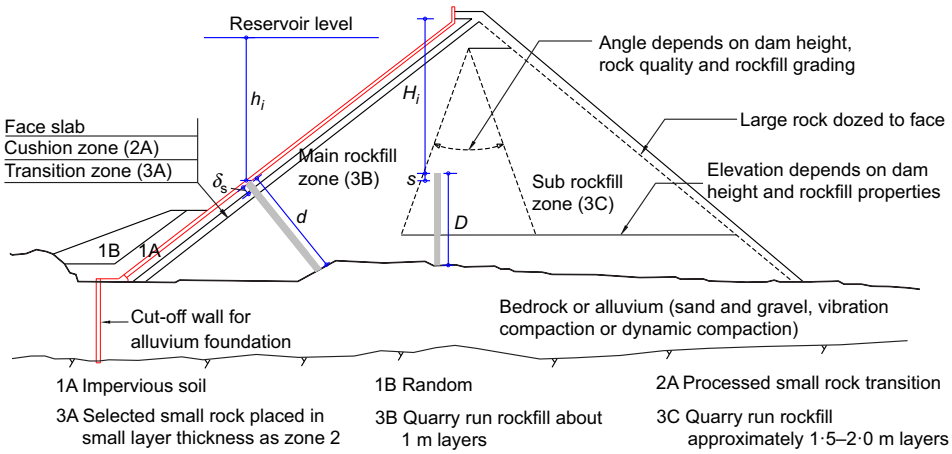

Fig. 1. Typical CFRD zoning (modified from Cooke & Sherard, 1987)

Downloaded by [UNIV OF ILLINOIS] on [05/02/20]. Copyright © ICE Publishing, all rights reserved.

crest settlement, respectively. Hunter (2003) suggested an empirical relation with E_t to estimate face slab deflection.

Case history database

This study uses a collection of monitoring and performance data from 87 CFRDs of sufficient monitoring data for behaviour assessment. Table 1 lists the construction details and maximum deformation measurements for the 87 in-service CFRDs built in 19 different countries in the past 50 years. The dam characteristics, construction details and behaviour information are collected. Most of the dams were constructed using compacted rockfill, and 16 were constructed using gravels as zone 3B or 3C. In total, 56 dams (cases 1–56) were constructed on rock foundation, and 31 dams (cases 57–87) were entirely or partially constructed on compressible foundation. Fig. 2 compares the percentages of the measuring period (from the completion of dam construction to the time of measurement), dam height and rockfill strength classification. The figure shows that the measuring period of most dams is less than 10 years, whereas for nearly half of them it is less than 5 years. The measuring period covers an overall range of 1–30 years. The height variation of most of the CFRDs is from 50 m to 150 m, with an overall range of 26–233 m. Nearly half of them were constructed using VH-strength rockfill. Table 1 shows that the intact strength of compacted rockfill is generally M to MH for CFRDs below 100 m; however, VH-strength rockfill is generally adopted for CFRDs built on alluvium foundation or with a height exceeding 100 m. The designed void ratio for dam construction is determined mainly by compaction test and similar projects. Table 1 indicates that the designed void ratios of rockfill for CFRDs vary over a range of 0·15–0·40. In particular, the void ratios for CFRDs using M-strength to MH-strength rockfill vary over a range of 0·15–0·25, which is smaller than those (0·15–0·30) for CFRDs using VH-strength rockfill.

Dam settlement and face slab deflection are the main parameters used to quantify the deformation characteristics of CFRDs. In this study, different settlements including crest, internal and ground settlements are dealt with. Crest settlement refers to the post-construction dam crest settlement, which contains the deformation at the stabilisation period before reservoir filling, during the reservoir-filling stage and after reservoir filling. Internal settlement refers to the dam body settlement during dam construction. Ground settlement refers to the foundation compression deformation at the end of dam construction. All of the dam settlements and face slab deflections are expressed in dimensionless forms normalised by dam height (% H, H: dam height). They all refer to the maximum cumulative deformation at the measurement time. Significant leakage exerts an economic effect in terms of water loss. Leakage rate refers to the amount of water exuded from the downstream of the dam and is measured using a weir installed downstream of the dam. The materials reviewed for the dams presented in Table 1 include published papers, unpublished reports and monitoring data. The CFRDs selected for this study are those with sufficient available and good-quality monitoring records. Data on crest settlements are from a geodetic monitoring system established during dam construction. Dams without adequate monitoring procedures or timely zero readings are disregarded to ensure comparability and quality of data. Data on internal and ground settlements are from electromagnetic settlement meters or hydraulic overflow settlement gauges installed in the dam body as construction proceeds. The settlements measured by the two installations are generally comparable (Kim *et al.*, 2014; Wen *et al.*, 2017). The reference (origin, 0 settlement) is taken at the time at which initial measurements are conducted (i.e. when the datum point for readings after construction is established). All of the selected internal and ground settlements possess adequate procedures and timely zero readings. Face slab deflections are mainly measured with an inclinometer. Several early cases that do not possess adequate procedures or timely zero readings have been modified in the source literature and can thus reasonably represent face slab deflection. The collected deflection data are of good quality and are comparable. The database represents CFRDs of different rockfill types and strengths, in valleys of different widths, on different foundation conditions and with dam heights ranging from 26 m to 233 m.

Complete information on foundation properties and ground settlements is unavailable in some of the 31 cases built on compressible foundation. The information is only available in 18 cases. Table 2 summarises the foundation properties and ground settlements of the 18 CFRDs built on an alluvium foundation (from Table 1). The thickness of most of the alluvium foundations ranges from 30 to 50 m, with an overall range of 24·3–110 m. The dry density of the alluvium foundation generally ranges from 2·0 to 2·2 g/cm^3. The alluvium deformation modulus (E_0) generally ranges from 40 to 60 MPa. E_0 is the ratio of vertical stress increment to the corresponding strain increment under unconfined conditions and is an important index for foundation compression deformation. This modulus reflects the capability of soil to resist elastoplastic deformation. The E_0 of most of the cases listed in Table 2 is estimated by a pressuremeter test. In this in situ test, E_0 is determined by a pressure–volume relationship curve on an empirical basis (CSHE, 2007). The E_0 of cases 71 and 78 is estimated by a dynamic penetration test. The empirical relationship between E_0 and the dynamic penetration index is used to determine E_0 (Li *et al.*, 2014). A plate-loading test is adopted to estimate the E_0 of case 83. In this in situ test, E_0 is determined by a pressure–settlement relationship curve (Hanna *et al.*, 1986). Pressuremeter and dynamic penetration tests can be applied to determine E_0 at different foundation depths, but the plate-loading test is mainly applicable to the determination of the modulus at a shallow foundation. E_0 has the same meaning and is given in the form of a range. Therefore, the moduli obtained by the different tests are roughly comparable. The E_0 of all cases used in the later analysis is measured in the same way (pressuremeter test).

POST-CONSTRUCTION CREST SETTLEMENT BEHAVIOUR

Post-construction crest settlement pattern

The post-construction deformations of CFRDs are caused by multiple mechanisms, including reservoir filling, collapse settlement, rockfill deterioration or weathering, reservoir fluctuation and long-term creep (Dounias *et al.*, 2012); among them, creep is responsible for the majority of long-term crest settlements (Wei *et al.*, 2010; Gan *et al.*, 2014). Crest settlement exhibits an obvious degree of dependency on the depth of bottom fill; thus, the settlement in the middle of the crest is always larger than that near the abutments of the crest (Kyrou *et al.*, 2005). Complete crest settlement information is unavailable in most of the 87 cases. Fig. 3(a) presents the measured crest settlement of 13 cases with complete crest settlement information as functions of time. Zero time is established at the completion of dam construction.

Nearly all of the dams fall within the range suggested by Clements (1984). CFRDs built on alluvium foundation exhibit a significantly larger crest settlement than dams built on rock foundation in the case of similar dam height,

Downloaded by [UNIV OF ILLINOIS] on [05/02/20]. Copyright © ICE Publishing, all rights reserved.

Table 1. Summary of case history data and behaviour measurements of 87 in-service CFRDs

No.	Dam	Country	Year*	H: m	CL: m	Foundation and depth	Rockfill source	IRS	e	SF (A/H^2)	IS:		CS		FD:		L: l/s	MP: year	Ref.†
											m	% H	m	% H	m	% H			
1	Tullabardine	Australia	1982	26	214	R	Sandstone	MH	0·23	8·1	—	—	0·02	0·08	—	—	0·75	12·8	R1, R2
2	Namgang	Korea	2001	34	1126	R	Gneiss	—	0·27	36·2	0·11	0·32	0·01	0·04	0·06	0·17	4	6	R3, R4
3	White Spur	Australia	1989	43	146	R	Tuff	VH	0·22	2·3	0·07	0·15	0·06	0·13	0·04	0·09	2	5·9	R3
4	Dongbok	Korea	1985	44·7	188	R	Granite	VH	0·27	3·5	0·33	0·74	0·04	0·09	0·04	0·09	—	7	R1
5	Buan	Korea	1996	50	410	R	Rhyolite	VH	0·25	7·3	0·44	0·88	0·20	0·41	—	—	—	11	R2, R3
6	Daegok	Korea	2006	52	190	R	Gneiss	VH	0·25	3·7	0·11	0·21	0·02	0·04	0·01	0·02	—	1	R2
7	Little Para	Australia	1977	53	225	R	Siltstone	M	—	—	—	—	0·15	0·29	—	—	19·2	22·6	R5
8	Jangheung	Korea	2005	53	403	R	Tuff	VH	0·28	10·7	0·44	0·83	0·02	0·04	0·03	0·06	—	1	R3, R4
9	Cheongsong (L)	Korea	2004	62	300	R	Granite	MH-VH	—	6·7	—	—	0·07	0·11	—	—	1·5	3·2	R1
10	Cabin creek	America	1969	64	350	R	Gneiss	MH	0·33	—	—	—	0·11	0·17	—	—	—	10	R6
11	Yongdam	Korea	2001	70	498	R	Shale	MH	0·32	8·8	0·35	0·50	0·12	0·17	0·01	0·01	—	6	R2
12	Sancheong (L)	Korea	2002	70·9	286	R	Granite	VH	0·27	6·3	0·27	0·37	0·09	0·13	0·01	0·01	—	6	R3
13	Chengbing	China	1989	74·6	325	R	Tuff	VH	0·28	2·8	0·28	0·38	0·10	0·13	0·19	0·25	33	10	R2
14	Bastyan	Australia	1983	75	430	R	Rhyolite	VH	0·23	3·4	0·17	0·23	0·05	0·07	0·07	0·09	5	9	R1, R7
15	Pushihe	China	2012	78·5	395	R	Tuff	VH	0·22	3·8	0·33	0·42	—	—	0·12	0·15	50	2	R8
16	Zeya	China	1998	78·8	312	R	Gravels	M-MH	0·25	3·7	0·40	0·51	0·12	0·15	0·14	0·18	—	15	R9
17	Mangrove creek	Australia	1981	80	380	R	Siltstone	MH	0·26	4·5	0·43	0·54	0·08	0·10	0·10	0·13	2·5	4	R1, R5
18	Pyonghwa (1st)	Korea	1988	80	590	R	Gneiss	VH	0·40	7·1	0·41	0·51	—	—	—	—	—	5	R3
19	Crotty	Australia	1990	83	240	R	Gravels	VH	0·20	1·9	0·18	0·22	0·06	0·07	0·05	0·06	32·5	9	R1, R3
20	Cokal	Turkey	2010	83	605	R	Limestone	MH	0·20	6·2	0·50	0·60	0·13	0·16	0·15	0·18	—	2	R10
21	Sugaroaf	Australia	1979	85	1050	R	Siltstone	MH	0·30	11·5	0·20	0·24	0·21	0·25	0·16	0·19	13	15	R1, R4
22	Sancheong (U)	Korea	2002	86·9	360	R	Granite	VH	0·27	3·1	0·39	0·44	0·30	0·35	0·01	0·01	—	6	R2, R4
23	Miryang	Korea	2001	89	535	R	Siltstone	—	0·18	6·8	0·43	0·48	0·09	0·10	0·16	0·18	9	6	R1, R4
24	Kotmale	Sri Lanka	1984	90	560	R	Gneiss	MH-VH	0·27	7·4	0·86	0·96	0·15	0·17	0·10	0·11	—	2·5	R5, R7
25	Cheongsong (U)	Korea	2004	90	400	R	Granite	VH	—	3·7	—	—	0·12	0·13	—	—	10	3·3	R1
26	Da'ao	China	1999	90·2	424	R	Sandstone	MH	0·21	3·6	0·92	1·02	0·21	0·23	0·23	0·25	61	8	R11
27	Wananxi	China	1995	93·8	210	R	Granite	MH	0·26	2·0	0·21	0·22	0·34	0·36	0·10	0·11	5·62	5	R3
28	Murchison	Australia	1982	94	200	R	Rhyolite	VH	0·23	1·9	0·20	0·21	0·08	0·09	0·09	0·10	2	18	R7, R11
29	Xibeikou	China	1989	95	222	R	Limestone	MH-VH	0·28	3·3	0·32	0·34	0·06	0·06	0·08	0·08	35·3	6	R2, R4
30	Bailey	America	1979	96	420	R	Sandstone	M	0·27	3·5	—	—	0·42	0·44	—	—	—	10	R6
31	Dongba	China	2006	105·9	467	R	Sandstone	M	—	—	2·30	2·18	—	—	—	—	—	—	R8
32	Cethana	Australia	1971	110	213	R	Quartzite	VH	0·26	2·5	0·50	0·46	0·18	0·16	0·17	0·16	7·5	30	R1,R13
33	Glevard	Iran	2012	110	275	R	Quartzite	VH	0·25	—	0·75	0·68	—	—	0·25	0·23	—	3	R14
34	Khao Laem	Thailand	1984	113	1000	R	Limestone	MH	0·29	8·3	1·37	1·21	0·19	0·17	0·13	0·12	53	14	R5,R7
35	Pankou	China	2011	114	292	R	Siltstone	VH	—	—	0·27	0·25	0·20	0·18	—	—	—	3	—
36	Turimiquire	Venezuela	1982	115	410	R	Limestone	MH	0·32	2·7	—	—	0·27	0·23	0·25	0·22	—	5	R6
37	Lower Pieman	Australia	1986	122	360	R	Dolerite	M	0·24	2·5	0·23	0·19	0·22	0·18	0·27	0·22	—	15	R5,R7
38	Shiroro	Nigeria	1984	125	560	R	Granite	VH	0·20	4·2	0·94	0·75	0·17	0·14	0·09	0·07	80	1·8	R5,R7
39	Cirata	Indonesia	1988	125	453	R	Andesite	M-MH	0·24	3·9	0·63	0·50	0·27	0·22	0·35	0·28	60	10	R6
40	Ita	Brazil	1999	125	880	R	Basalt	MH-VH	0·31	7·0	—	—	0·60	0·48	0·51	0·41	200	4	R1, R5
41	Golillas	Colombia	1978	127	107	R	Gravels	VH	0·24	0·9	0·39	0·31	0·05	0·04	0·16	0·13	385	7	R1, R3
42	Yinzidu	China	2004	129·5	276	R	Gravels	MH-VH	0·21	2·1	1·10	0·85	0·12	0·09	0·20	0·15	—	5	R15
43	Gongboxia	China	2002	132·2	429	R	granite	VH	0·17	2·5	0·35	0·26	0·15	0·11	0·18	0·14	—	10	R16

Downloaded by [UNIV OF ILLINOIS] on [05/02/20]. Copyright © ICE Publishing, all rights reserved.

44	Kurtun	Turkey	1999	133	300	R	Limestone	MH	0·22	2·2	2·02	1·50	0·11	0·08	—	—	—	1	R17, R18
45	Segredo	Brazil	1993	145	720	R	Basalt	MH-VH	0·37	4·1	2·22	1·53	0·23	0·16	0·34	0·23	45	8	R2, R5
46	Dongjing	China	2009	149·5	566	R	Sandstone	VH	0·19	3·7	1·78	1·19	—	—	0·60	0·40	—	3	R15
47	Mesochora	Greece	1995	150	340	R	Limestone	M	0·23	1·6	2·10	1·40	0·22	0·15	0·33	0·22	—	5	R19
48	Malutang	China	2009	154	493	R	granite	VH	0·19	2·4	1·50	0·97	0·25	0·16	0·28	0·18	80	3	R20
49	Zipingpu	China	2006	156	664	R	Limestone	VH	0·26	4·8	0·71	0·46	0·21	0·13	0·25	0·16	90	6	R21
50	Jilintai	China	2006	157	445	R	Tuff	VH	0·23	3·1	0·59	0·38	—	—	0·24	0·15	—	7	R15
51	Foz do Areia	Brazil	1980	160	828	R	Basalt	MH-VH	0·33	5·4	3·58	2·34	0·21	0·13	0·78	0·49	70	20	R1, R3
52	Tiaoshengqiao	China	2000	178	1104	R	Limestone	M-VH	0·31	4·9	3·28	1·84	1·06	0·60	1·14	0·64	70	1·5	R22
53	Hongjiadu	China	2005	179·5	428	R	Limestone	VH	0·20	2·4	1·24	0·69	0·32	0·18	0·35	0·19	140	6	R15
54	Sanbanxi	China	2007	185	423	R	Gravels	MH	0·22	2·5	1·05	0·57	0·17	0·10	0·17	0·10	100	5	R15
55	Bakun	Malaysia	2007	205	740	R	Sandstone	VH	0·20	2·8	2·27	1·10	—	—	0·80	0·39	—	4	—
56	Shuibuya	China	2007	233	675	R	Limestone	VH	0·22	2·3	2·30	0·98	0·35	0·15	0·28	0·12	20	3	R23
57	Pappadai	Italy	1992	27	890	G, 50 m	Limestone	VH	—	—	0·07	0·26	0·01	0·04	—	—	—	7	R24
58	Lianghui	China	1997	35·4	410	G, 25 m	Tuff	VH	0·23	8·8	0·21	0·59	0·08	0·23	0·06	0·17	130	8	R25
59	Chusong	China	1998	40	308	G, 35 m	Gravels	MH	0·21	13·7	0·16	0·40	0·04	0·10	—	—	28	9	R25
60	Meixi	China	1998	41	652	G, 30 m	Tuff	MH	—	22·2	0·20	0·48	0·08	0·20	0·13	0·32	—	10	R25
61	Kekeya	China	1981	42	123	G, 37·5 m	Gravels	M	—	6·8	—	—	0·03	0·07	—	—	20	7	R25
62	Tongjiezi	China	1992	48	434	G, 71 m	Basalt	VH	—	—	0·45	0·94	—	—	0·12	0·25	—	8	R25
63	Dahe	China	1998	50·8	168	G, 37 m	Limestone	M	0·21	4·1	0·25	0·49	0·12	0·23	0·13	0·25	—	8	R25
64	Shuangxikou	China	2009	52·1	426	G, 15·4 m	Tuff	MH	0·20	10·2	0·46	0·94	—	—	0·17	0·32	—	2	R9
65	Pichi-Picun Leufu	Argentina	1999	54	1045	G, 28 m	Gravels	M	0·19	9·1	0·50	0·90	0·13	0·24	0·16	0·30	18	8	R19
66	Hanpingzui	China	2006	57	202	G, 45 m	Gravels	VH	0·22	4·0	0·33	0·58	0·12	0·21	0·13	0·23	95	5	R25
67	Kangaroo Creek	Australia	1969	60	178	R, G, 20 m	Shale	M-MH	—	—	—	—	0·12	0·19	—	—	2·5	26	R4, R5
68	Hengshanba	China	2006	70·2	210	G, 72·3 m	Tuff	MH	0·23	2·9	0·50	0·71	0·17	0·24	0·18	0·25	180	5	R8
69	Tianhuangping	China	1998	72	503	WR, 35 m	Tuff	MH	—	—	0·64	0·89	—	—	—	—	—	—	R26
70	Mackintosh	Australia	1981	75	465	WR	Sandstone	M-MH	0·24	4·9	0·48	0·64	0·24	0·32	0·49	0·65	9	19	R7, R12
71	Puclaro	Chile	1999	83	640	G, 113 m	Gravels	M	0·20	2·4	0·67	0·81	0·11	0·13	0·12	0·14	—	5	R20
72	Laodukou	China	2009	96·6	172	G, 29·6 m	Gravels	MH	—	2·1	0·34	0·35	—	—	0·11	0·11	—	2	—
73	Nalan	China	2005	109	333	G, 24·3 m	Gravels	MH	0·19	2·9	0·31	0·28	0·16	0·15	0·16	0·15	95	6	R25
74	Chahanwusu	China	2009	110	338	G, 46·7 m	Gravels	VH	0·17	3·7	0·53	0·48	0·22	0·20	0·30	0·27	15	2	R27
75	Miaojiaba	China	2011	110	348	G, 48 m	Tuff	VH	0·20	2·5	0·91	0·83	0·28	0·26	0·30	0·27	—	1	R27
76	Duonuo	China	2012	112·5	220	G, 35 m	Sandstone	VH	0·21	2·2	1·10	0·98	0·33	0·30	0·23	0·20	—	2	R27
77	Santa Juana	Chile	1995	113·4	390	G, 30m	Gravels	M	—	3·1	—	—	0·01	0·01	—	—	50	4	R19
78	Potrerillos	Argentina	2003	116	395	G, 35 m	Limestone	VH	0·21	3·1	0·82	0·70	0·29	0·25	0·30	0·26	180	6	R6
79	Reece	Australia	1986	122	374	G	Dolerite	VH	0·24	—	0·23	0·19	0·22	0·18	0·26	0·21	1	15	R1, R2
80	Shanxi	China	2000	132·5	448	G, 24 m	Tuff	VH	0·20	3·4	0·95	0·72	—	—	0·20	0·15	—	6	R9
81	Jiudianxia	China	2008	136	232	G, 56 m	Limestone	VH	0·17	2·0	1·24	0·91	0·42	0·31	0·84	0·62	136	3	R28
82	Los Caracoles	Argentina	2009	136	605	G, 28 m	Limestone	MH	0·23	4·5	1·01	0·80	0·38	0·28	0·41	0·30	200	4	—
83	Alto Anchicaya	Columbia	1974	140	260	G, 34 m	Hornfels	VH	0·22	1·1	0·63	0·45	0·17	0·12	0·16	0·11	180	10	R5, R12
84	Xingo	Brazil	1994	150	850	R, G, 41 m	Granite	M-VH	0·28	6·0	2·90	1·93	0·53	0·35	0·51	0·34	140	6	R4, R7
85	Salvajina	Columbia	1983	154	362	G, R, 30 m	Gravels	MH-VH	0·21	2·4	0·30	0·20	0·09	0·06	0·06	0·04	80	7·5	R3, R7
86	Tankeng	China	2008	162	507	G, 30 m	Tuff	VH	—	3·7	0·81	0·50	0·15	0·09	0·17	0·10	80	5	R15, R25
87	Aguamilpa	Mexico	1993	187	475	R, G	Gravels	VH	0·18	3·9	—	—	0·34	0·18	0·32	0·17	160	7	R3, R7

Note: *H*, dam height; CL, crest length; R, rock foundation; G, alluvium (sand and gravel) foundation; WR, weathered rock foundation; IRS, intact rockfill strength classification; *e*, void ratio; SF, valley shape factor; *A*, upstream slope face area; IS, maximum internal settlement at the end of construction; CS, maximum crest settlement; FD, maximum post-construction face slab deflection; *L*, leakage after reservoir filling; MP, measuring period.
*The heading means the year of end of dam construction.
†R1, Won & Kim (2008); R2, Kim *et al*. (2014); R3, Kim & Kim (2008); R4, Seo *et al*. (2009); R5, Cooke (1984); R6, ICOLD (2004); R7, Pinto & Marques (1998); R8, Li (2007); R9, Li *et al*. (2001); R10, Arici (2011); R11, Xing *et al*. (2006); R12, Sherard & Cooke (1987); R13, Khalid *et al*. (1990); R14, Mahabad *et al*. (2014); R15, Li (2011); R16, Wang *et al*. (2014); R17, Özkuzukiran *et al*. (2006); R18, Gurbuz (2011); R19, Hunter (2003); R20, Jia & Chi (2015); R21, Xu *et al*. (2015). R22, Zhang *et al*. (2004); R23, Zhou *et al*. (2011); R24, Lollino *et al*. (2005); R25, CSHE (2007); R26, Wang & Liu (2005); R27, Li *et al*. (2014); R28, Gan *et al*. (2014).

Downloaded by [UNIV OF ILLINOIS] on [05/02/20]. Copyright © ICE Publishing, all rights reserved.

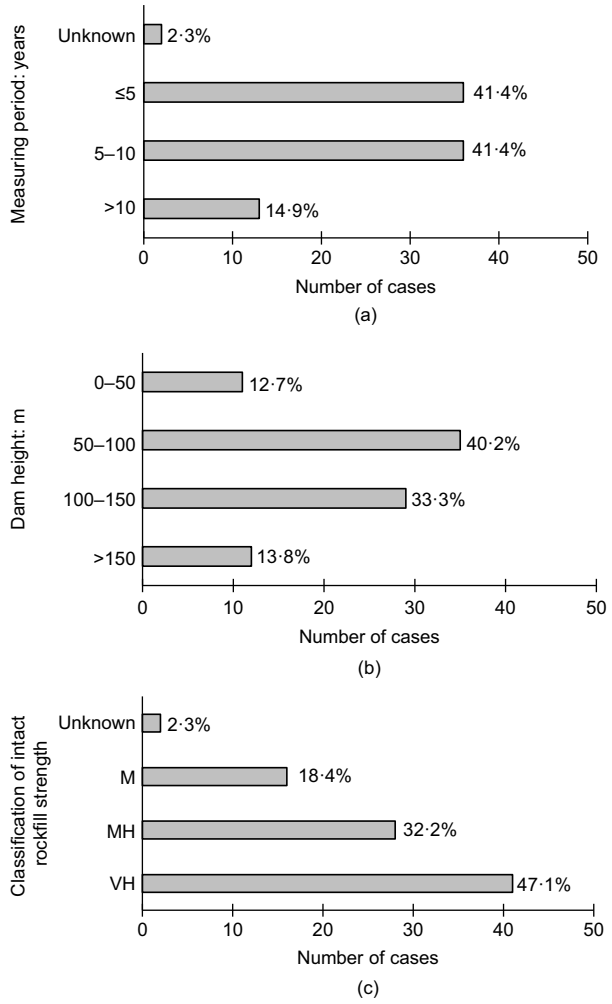

Fig. 2. Statistics of: (a) measuring period; (b) dam height; and (c) classification of intact rockfill strength

rockfill strength and valley shape. For example, the crest settlement after reservoir filling of the Miaojiaba Dam on alluvium is 0·1% H larger than that of the Cethana Dam on bedrock. Similarly, dams constructed using low-strength rockfill exhibit a significantly larger crest settlement than dams constructed using high-strength rockfill in the case of similar dam height, foundation condition and valley shape. For example, the crest settlement of the Turimiquire Dam (MH-strength rockfill) after reservoir filling is 0·09% H larger than that of the Cethana Dam (VH-strength rockfill). These results suggest that crest settlement is significantly influenced by rockfill strength and foundation conditions. Large crest settlements are observed for CFRDs built on alluvium foundation and constructed using low-strength rockfill, and these dams need much time to reach a small crest settlement rate. For example, under the combination of alluvium foundation and low-strength rockfill, the Mackintosh Dam shows a significantly large crest settlement.

The crest settlement of a CFRD comprises time-dependent deformation and deformation on the first reservoir filling. Won & Kim (2008) reported that 10–40% (23% on average) of the total crest settlement occurs during reservoir filling. Lawton & Lester (1964) stated that 85% of the total crest settlement occurs during the first year after the commencement of reservoir filling. Gikas & Sakellariou (2008) reported that 60% of the total crest settlement of a rockfill dam occurs prior to the completion of reservoir filling. The reservoir filling effect is often observed as an acceleration in crest settlement rate, thereby causing a significant crest settlement increment. Most of the cases lack data for the deformation caused by reservoir filling. Fig. 3(b) shows the ratio of the crest settlement and face slab deflection of CFRDs built on alluvium foundation and with available data on reservoir filling to total deformation. Cases built on rock foundation are excluded in Fig. 3(b) but are analysed separately to compare the ratio of deformation on reservoir filling to total deformation under different foundation conditions. Approximately 10–60% (27% on average) of the total crest settlement occurs during the reservoir filling for CFRDs built on alluvium foundation, and these values

Table 2. Summary of foundation characteristics of 18 CFRDs built on alluvium foundation

No.*	Dam	Country	Year	H: m	Foundation properties				Ground settlement:†	
					Ground condition	T: m	Dry density: g/cm^3	E_0: MPa	m	% T
57	Pappadai	Italy	1992	27	Gravels	50	2·10–2·20	50–65	0·25	0·50
58	Lianghui	China	1997	35·4	Gravels	25	2·00	40–55	0·16	0·64
59	Chusong	China	1998	40	Sand and gravel	35	2·10–2·15	50–55	0·29	0·83
60	Meixi	China	1998	41	Sand and pebble	30	2·00	—	0·21	0·70
61	Kekeya	China	1981	42	Sand and gravel	37·5	—	60	0·30	0·80
63	Dahe	China	1998	50·8	Gravels	37	2·05	55–60	0·33	0·89
66	Hanpingzui	China	2006	57	Sand and gravel	45	2·10–2·20	55–60	0·44	0·98
68	Hengshanba	China	2006	70·2	Sand and gravel	40	2·15	—	0·35	0·88
71	Puclaro	Chile	1999	83	Sand and gravel	113	2·00–2·15	50–60	—	—
72	Laodukou	China	2009	96·6	Sand and gravel	29·6	2·00	50–60	0·18	0·61
73	Nalan	China	2005	109	Gravels	24·3	2·19	33–45	0·22	1·32
74	Chahanwushu	China	2009	110	Sand and gravel	46·7	2·14	45–55	0·35	0·75
75	Miaojiaba	China	2011	110	Sand and gravel	48	2·15–2·20	60–65	0·45	0·94
76	Duonuo	China	2012	112·5	Crushed gravel	35	2·17	45–55	0·37	1·06
77	Santa Juana	Chile	1995	113·4	Sand and gravel	30	2·10	—	—	—
78	Potrerillos	Argentina	2003	116	Gravels	35	2·00–2·10	60–65	—	—
81	Jiudianxia	China	2008	136	Sand and gravel	56	1·95–2·12	40–60	0·53	0·95
83	Alto Anchicaya	Columbia	1983	154	Sand and gravel	34	2·20	55–60	—	—

Note: H, dam height; T, alluvium thickness; E_0, alluvium deformation modulus.
*The case numbers are from Table 1.
†The heading refers to the ground settlement at the end of dam construction.

Downloaded by [UNIV OF ILLINOIS] on [05/02/20]. Copyright © ICE Publishing, all rights reserved.

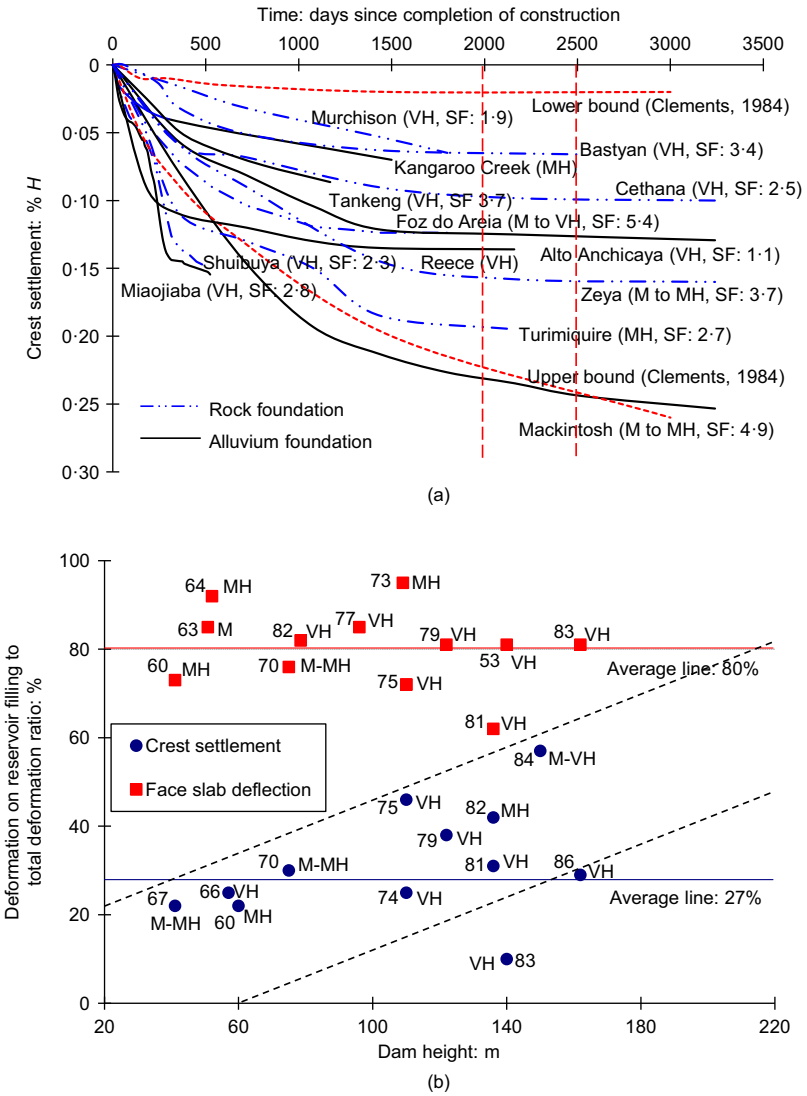

Fig. 3. (a) Measured crest settlement of 13 cases as functions of time; (b) ratio of crest settlement and face slab deflection built on alluvium foundation on reservoir filling to total deformation. The serial numbers indicate the numbers of dams as shown in Table 1

are larger than the average result of 22% for CFRDs built on rock foundation. The effect of reservoir filling on crest settlement increases with dam height and the decrease in rockfill strength. For dams constructed using M-strength to MH-strength rockfill, the crest settlement increment caused by reservoir filling accounts for 32% on average of the total crest settlement; this value is approximately 7% larger than that for a VH-strength rockfill dam. The crest settlement always shows an 'S'-shaped curve as a function of time under the effect of water load. The pattern in Fig. 3(a) is unclear because the difference in time span and dam deformation is large.

Many crest settlement records of rockfill dams show continually increasing settlements after several decades of operation. The crest settlement rate for a rockfill dam creates a straight line on a log scale (Clements, 1984; Hunter, 2003; Dounias *et al.*, 2012). Gikas & Sakellariou (2008) reported that the crest settlement of a rockfill dam requires 10–20 years to reach a small settlement rate. Dounias *et al.* (2012) found that crest settlement rate is high and is visibly influenced by the reservoir fluctuations in the first 10 years, and the rate reduces rapidly in the next 10 years. The crest settlement rate of a CFRD differs from that of an earth core rockfill dam, given that no consolidation exists in the core owing to the excess pore pressure dissipation. Sherard & Cooke (1987) reported that the crest settlement rate of a CFRD is low and decreases rapidly after the first few years. Hunter (2003) reported that crest settlement converges to a final value after 6 years of operation. Fig. 3(a) shows that crest settlement increases with time after the completion of dam construction, but the settlement rate decreases gradually. The settlement rate reaches a near-constant value that corresponds to an average settlement rate of less than 1 mm/year 2000–2500 days (approximately 5–6 years) after dam construction. Crest settlement and the time for dams to reach a small settlement rate differ for each dam. Deformation is influenced mainly by rockfill and foundation characteristics, construction method and valley shape.

Statistical analysis on crest settlement

Dam crest is generally given a camber of 1·0% H (crest settlement reservation) to accommodate post-construction crest settlement (Gurbuz, 2011). The value of crest settlement reservation is usually determined by settlement calculation, settlement observation during construction and engineering analogy method. Dam settlement depends on void ratio and rockfill characteristics under the action of dam weight and water load. CFRD behaviour is affected by many factors, including construction methods (e.g. compaction, lift

Downloaded by [UNIV OF ILLINOIS] on [05/02/20]. Copyright © ICE Publishing, all rights reserved.

Table 3. Range of crest settlement, face slab deflection and internal settlement

IRS	H: m	Crest settlement: % H				Face slab deflection: % H				Internal settlement: % H	
		< 5 years		> 5 years		< 5 years		> 5 years		R	G
		R	G	R	G	R	G	R	G		
VH	<50	<0·04	0·04–0·10	0·05–0·09	0·04–0·23	0·02–0·05	0·05–0·10	0·05–0·09	0·07–0·20	0·05–0·15	0·2–0·6
	50–100	0·04–0·13	0·10–0·20	0·07–0·15	0·10–0·25	0·05–0·10	0·10–0·23	0·05–0·15	0·10–0·25	0·20–0·50	0·5–0·8
	100–150	0·10–0·18	0·12–0·30	0·10–0·20	0·12–0·30	0·10–0·20	0·10–0·27	0·13–0·20	0·10–0·27	0·25–0·80	0·5–1·0
	>150	0·13–0·20	0·18–0·35	0·13–0·25	0·18–0·35	0·12–0·30	0·10–0·35	0·15–0·30	0·17–0·35	0·50–1·10	1·0–1·5
M to MH	<50	0·05–0·10	0·10–0·15	0·08–0·10	0·17–0·23	0·05–0·17	0·10–0·20	0·10–0·20	0·10–0·20	0·30–0·50	0·4–0·8
	50–100	0·10–0·17	0·13–0·24	0·15–0·20	0·19–0·26	0·10–0·20	0·11–0·25	0·10–0·25	0·15–0·30	0·50–1·00	0·5–1·2
	100–150	0·17–0·30	0·10–0·35	0·17–0·30	0·10–0·35	0·16–0·25	0·20–0·30	0·16–0·28	0·20–0·35	0·50–1·50	1·0–1·8
	>150	0·15–0·35	0·20–0·35	0·20–0·35	0·20–0·35	0·20–0·35	0·20–0·40	0·20–0·38	0·20–0·43	1·00–2·00	1·0–2·5

Note: IRS, intact rockfill strength classification; H, dam height; R, rock foundation; G, alluvium foundation.

thickness and water content), material properties (e.g. mineralogy, intact rock strength and gradation), geometric features (e.g. zone design, valley shape and foundation characteristics) and load and boundary conditions (e.g. water level fluctuation and rainfall). Fell *et al.* (2005) attempted to group post-construction crest settlement on the basis of several factors, but they only drew a few general conclusions because of the scatter of reported data. They reported that the magnitude and rate of crest settlement and face deflection can vary by one to two orders of magnitude because of the numerous influencing factors of dam behaviour. Additional factors should be considered to obtain clear rules of the database.

Table 3 summarises the crest settlement, face slab deflection and internal settlement of CFRDs on the basis of Table 1. Large deformations are expected from increasing dam height and measuring period, low-strength rockfill and CFRDs built on an alluvium foundation. However, a broad range of deformations within different rockfill strengths and height groupings are observed. Attempts to incorporate other influencing factors of dam behaviour, such as rockfill gradation, construction method and valley shape, result in a high degree of data variability. Preliminary estimates of dam behaviour in terms of rockfill strength, dam height, measuring period and foundation conditions are presented in Table 3. Low values are generally applicable to dams within any range with good-quality rockfill and narrow valley.

Figure 4 presents the crest settlement measured in the 87 cases with respect to dam height for different rockfill strengths and foundation characteristics, as well as the summarised range. The ranges of crest settlement of other investigators are also included in Fig. 4 for comparison. Approximately 90% of the case histories exhibit crest settlements of 0·4% H or smaller; however, the Ita Dam (0·48% H), Tianshengqiao Dam (0·60% H) and Bailey Dam (0·44% H) exhibit large crest settlements. Such large settlements may be due to the complex zoning and discontinuous gradation of the Ita Dam, the large height (178 m) of the Tianshengqiao Dam and the low-strength rockfill (25 MPa) of the Bailey Dam. Table 3 and Fig. 4 indicate that crest settlements are slightly larger at dams with a measuring period of more than 5 years than those at dams with a measuring period of less than 5 years. This observation can be explained by the previous analysis that, although the dam crest deforms for a long time, most deformations occur within the first few years after dam construction (5–6 years). Crest settlement is large at dams constructed using low-strength rockfill. The difference in the upper range for a measuring period of less than 5 years between dams on rock foundation constructed using VH-strength rockfill and M-strength rockfill is approximately 0·1% H. The crest settlements of CFRDs built on alluvium foundation are significantly larger than those of CFRDs built on rock foundation. Under the influence of foundation deformation, the crest settlement of dams with VH-strength rockfill on alluvium foundation is 0·06% H larger than that of dams on rock foundation in 5 years on average. The difference in the upper range exceeds 0·1% H, which indicates that the effect of foundation characteristics on dam settlement is more obvious than that of rockfill strength. These results imply that crest settlement is significantly influenced by rockfill strength and foundation characteristics.

The range obtained from the case data coincides with the report of Won & Kim (2008) to a certain extent. However, the previous range for M-strength to MH-strength rockfill and the range suggested by Seo *et al.* (2009) obviously overestimate crest settlement. The range of less than 0·25% H suggested by other investigators underestimates crest

Downloaded by [UNIV OF ILLINOIS] on [05/02/20]. Copyright © ICE Publishing, all rights reserved.

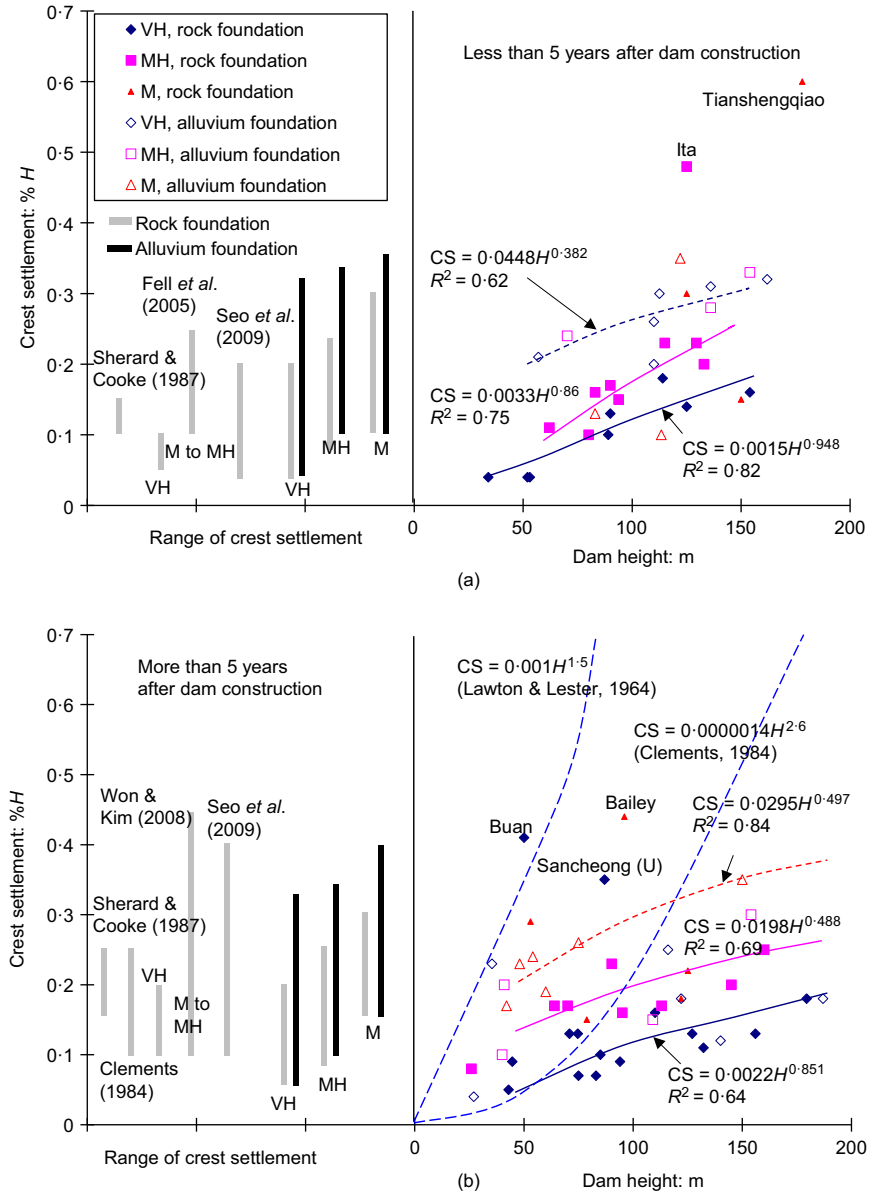

Fig. 4. CFRD crest settlement with respect to dam height in (a) less than 5 years and (b) more than 5 years

settlement and agrees only in the cases of CFRDs built on rock foundation. The reason may be that these ranges are derived mainly from a statistical analysis of dams on rock foundation.

Several empirical prediction methods have been proposed to predict the crest settlement of CFRDs. Clements (1984) conducted a best-fit analysis of the data of 68 dams and suggested adopting $CS = aH^b$ to predict crest settlement, where a and b are constants (a is 0·0002 at the end of reservoir filling and 0·0000014 after 10 years of service, and b is 1·1 at the end of reservoir filling and 2·6 after 10 years of service). Sowers *et al.* (1965) investigated the crest settlement of 14 dams and suggested using $CS = cH(\log t_2 - \log t_1)/100$ to determine crest settlement in time periods t_1 to t_2, where t_1 and t_2 are times in the month using the mid-point of the construction period as zero time. Coefficient c increases with time and has values between 0·2 and 1·05, and its general value is 1·0 when the time period is more than 10 years. After performing a best-fit analysis of data from 11 dams, Lawton & Lester (1964) obtained the relationship of $CS = 0{\cdot}001H^{1{\cdot}5}$ in predicting total crest settlement when settlement rate is less than 0·02% H per year. These existing methods are based on simple empirical relationships of crest settlement with dam height or time without considering many other influencing factors (e.g. material characteristics, construction method and foundation characteristics) of dam behaviour. These methods are the old methods, which generally are not in use. Additional factors should be considered in prediction calculations to reach a reliable prediction method. Several suggested empirical relationships are obtained by regression analysis for several groups of rockfill strengths and foundation conditions in Fig. 4. However, an empirical relationship cannot be obtained for other conditions given the different numbers of cases. Outliers to the general trend (Ita, Buan, Sancheong (U)) are excluded from the correlations. The suggested empirical relationships between crest settlement and dam height in the form of a power function are summarised in Table 4. The data within each group of rockfill strength and foundation conditions show a reasonable fit, as indicated by the high regression coefficients. The factors incorporated into the deformation prediction include measuring period, rockfill strength, foundation conditions and dam height. A clear tendency of increasing crest settlement with dam height is observed. The empirical relationship curves for the first 5 years and for the period more than 5 years are similar, but the crest settlement values

Downloaded by [UNIV OF ILLINOIS] on [05/02/20]. Copyright © ICE Publishing, all rights reserved.

Table 4. Suggested empirical relationships for crest settlement, internal settlement and face slab deflection

IRS and foundation	Crest settlement	Internal settlement	Face slab deflection
VH, R	$CS = 0{\cdot}0015H^{0{\cdot}948}$, $R^2 = 0{\cdot}82$, <5 years, 8 cases	$IS = 0{\cdot}0154H^{0{\cdot}686}$, $R^2 = 0{\cdot}71$, 23 cases	$FD = 0{\cdot}00000186H^{2{\cdot}292}$, $R^2 = 0{\cdot}62$, <5 years, 5 cases
	$CS = 0{\cdot}0022H^{0{\cdot}851}$, $R^2 = 0{\cdot}64$, >5 years, 13 cases		$FD = 0{\cdot}00506H^{0{\cdot}677}$, $R^2 = 0{\cdot}63$, >5 years, 14 cases
MH, R	$CS = 0{\cdot}0033H^{0{\cdot}86}$, $R^2 = 0{\cdot}75$, <5 years, 8 cases	$IS = 0{\cdot}0032H^{1{\cdot}261}$, $R^2 = 0{\cdot}79$, 9 cases	$FD = 0{\cdot}00026H^{1{\cdot}392}$, $R^2 = 0{\cdot}66$, <5 years, 10 cases
	$CS = 0{\cdot}0198H^{0{\cdot}488}$, $R^2 = 0{\cdot}69$, >5 years, 8 cases		$FD = 0{\cdot}00035H^{1{\cdot}344}$, $R^2 = 0{\cdot}66$, >5 years, 7 cases
VH, G	$CS = 0{\cdot}0488H^{0{\cdot}382}$, $R^2 = 0{\cdot}62$, <5 years, 6 cases	$IS = 0{\cdot}0525H^{0{\cdot}568}$, $R^2 = 0{\cdot}65$, 13 cases	—
M, G	$CS = 0{\cdot}0295H^{0{\cdot}497}$, $R^2 = 0{\cdot}84$, >5 years, 8 cases	—	—

Note: IRS, intact rockfill strength classification; R, rock foundation; G, alluvium foundation; R^2, coefficient of determination.

for the first 5 years are generally smaller than those for the period more than 5 years. Fig. 4 and Table 4 show that the significant influencing factors of crest settlement are dam height, intact strength and foundation conditions. The suggested empirical relationships are derived from a good-quality data set and consideration of the significant influencing factors of deformation behaviour; therefore, they can be used as guides for the purpose of prediction.

Figure 5 compares the predicted crest settlement of 15 case histories by use of several existing empirical methods and the suggested relationships in Table 4 with the measured values of a measuring period of more than 10 years. These 15 cases, which are selected from the study of Hunter (2003) and are not part of the data used in regression analysis, possess different rockfill strengths and foundation conditions. Figs 4(b) and 5 show that the Lawton & Lester equation significantly overestimates crest settlement and can thus be used as the upper limit of post-construction crest settlement. On the contrary, the Sowers equation significantly underestimates crest settlement and can thus be used as a lower limit. Fig. 4(b) shows that the Clements equation agrees only with the data for dams with a height of less than 100 m and VH-strength rockfill on rock foundation to a certain extent. The crest settlements predicted using the existing empirical equations exhibit a significant difference from the observed values. The predicted results present a poor correlation for two reasons. First, the methods are based on simple empirical relationships of crest settlement with dam height or time. Second, the improvement in the compaction technique and the adoption of good-quality rockfill for modern CFRDs can help reduce post-construction deformation. The calculated mean, standard deviation and minimum root-mean-square error between measured and predicted crest settlements for the suggested relationships are 0·071, 0·075 and 0·041, respectively. The mean value and root-mean-square error imply that the predicted results using the suggested relationships in this study significantly agree with the measurements, unlike previous empirical methods. The suggested empirical relationships provide a reasonable basis for estimating crest settlement. Kim & Kim (2008) developed an artificial neural network model to predict post-construction crest settlement by use of 30 cases of field data (21 were used for training and nine for testing). The model considers H, e and E_v. The network was trained using a back-propagation algorithm. A three-layer artificial neural network model with one input–one hidden–one output layer was used. The number of hidden neurons was set to a reasonable value using a

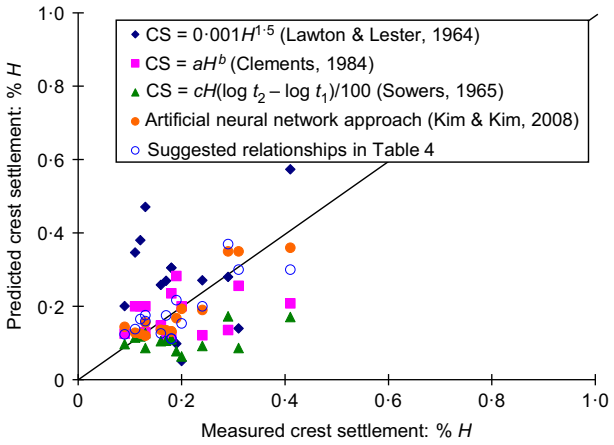

Fig. 5. Comparison of the predicted crest settlement of 15 cases by adopting prediction methods and artificial neural network with measured values (more than 10 years)

Downloaded by [UNIV OF ILLINOIS] on [05/02/20]. Copyright © ICE Publishing, all rights reserved.

cross-validation approach. Fig. 5 shows that the predicted results agree to a considerable extent with the measured data. The calculated mean, standard deviation and root-mean-square error between measured and predicted crest settlements for the artificial neural network model are 0·072, 0·073 and 0·038, respectively. The artificial neural network model is an alternative method for predicting crest settlement.

Effect of rockfill strength

The effect of rockfill strength on dam deformation is further analysed. Cases built on rock foundation and with a measuring period of more than 5 years are selected in the analysis to avoid the interference of other influencing factors (e.g. foundation characteristics and measuring period) and clearly show the effect of rockfill strength on dam deformation. Fig. 6 presents the crest settlement more than 5 years after dam construction measured in CFRDs built on rock foundations with respect to the classification of rockfill strength. Crest settlement is large for dams constructed using low-strength rockfill. Crest settlement constructed using M-strength rockfill is 2·1 times that using VH-strength rockfill, on average. Similarly, Hunter & Fell (2003) found that the total crest settlement constructed using M-strength to MH-strength rockfill at 10 years is 2 times that using VH-strength rockfill on average. These observations can be explained in that weak rockfill can easily yield large post-construction deformation because of the breakdown of particles. Nearly all of the cases fall within the trend lines, except the Sancheong (U) Dam and Buan Dam, which exhibit significantly larger crest settlements. This result may be attributed to the inadequate compaction and wide river valley of the Buan Dam and the discontinuous particle size distribution and complex zoning of the Sancheong Dam. The crest settlement of some dams with a measuring period of less than 5 years exhibits large values, such as that of the Ita Dam (0·41% H) and Tianshengqiao Dam (0·60% H). Such large crest settlement may be due to inadequate compaction, large height and discontinuous gradation. Fig. 6 shows that the cases of CFRDs constructed using gravels exhibit small deformation because of the large deformation modulus and low void ratio of the compacted gravels.

INTERNAL SETTLEMENT BEHAVIOUR

Internal settlement pattern

Settlement of CFRD during construction is governed by two main mechanisms: one is contact breakage among grains, and the other is block reorientation within the dam; settlement is affected by mineralogy, gradation, grain shape and grain size of the rockfill materials (Saboya & Byrne, 1993). The increase in vertical stress and compaction of materials results in an increase in relative density and a decrease in void ratio of the rockfill. The maximum internal settlement of a typical CFRD generally occurs near the centre of the dam body during construction as well as near the middle of the upstream face; internal settlement gradually decreases as the downstream face is approached during reservoir filling (Özkuzukiran *et al.*, 2006; Xu *et al.*, 2015).

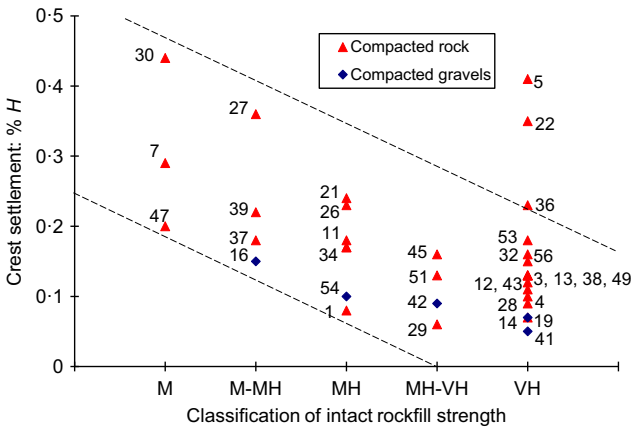

Fig. 6. Crest settlement (more than 5 years) of CFRDs built on rock foundations with respect to classification of intact rockfill strength

Figure 7(a) shows the distribution of the observed internal settlement for the Chahanwusu Dam at the end of its construction. A maximum internal settlement of 0·53 m is measured 30 m above the dam base during construction, and 0·25 m near the bottom of the upstream face during reservoir filling. The maximum internal settlements during construction and reservoir filling move downward under the effect of the foundation. Fig. 7(b) shows the evolution of the maximum internal settlement of 13 cases with time. These cases possess reliable and complete internal settlement information. The time and duration of construction of each dam differ. To unify the construction stage of the dam and allow comparability of data, the time at the end of reservoir filling of each case is set as the reference time in Fig. 7(b). The figure does not contain a complete construction stage of a few cases. Zhou *et al.* (2011) argued that more than 85% of the total internal settlement occurs during construction in some positions of the Shuibuya Dam. Fig. 7(b) shows that internal settlement increases rapidly during construction and over 80% of the total internal settlement occurs prior to the completion of the reservoir filling. After reservoir filling, internal settlement increases over time because of rockfill creep; however, settlement increments inside dams become very small with a settlement rate of less than 2 mm/month on average. Most maximum internal settlements are less than 1·0% H, except those for three dams with a height of more than 150 m.

Statistical analysis on internal settlement

Figure 8(a) presents the internal settlement measured in the 87 cases with respect to dam height during dam construction for different rockfill strengths and foundation characteristics, as well as the summarised range. Approximately 86% of the case histories exhibit internal settlements of less than 1·0% H, except a few points with a dam height of over 150 m, such as the Foz do Areia Dam (2·34% H), Tianshengqiao Dam (1·84% H) and Xingo Dam (1·93% H). Deformation control methods and elimination measures should be considered to ensure the stability of high dams (more than 150 m). When dam height and alluvium thickness are considered simultaneously, most of the internal settlements of CFRDs built on an alluvium foundation are less than 0·8% of the total height. Table 3 and Fig. 8(a) show that, similarly to crest settlement, internal settlement is large at dams constructed using low-strength rockfill and built on an alluvium foundation. The internal settlement of dams on rock foundation constructed using MH-strength rockfill is 1·4 times that of VH-strength rockfill dams on average. Under the influence of foundation deformation, the internal settlement of dams on alluvium foundation is 0·12% H larger than that of dams on rock foundation on average. Internal settlement gradually increases with dam height. These results indicate that internal settlement is significantly influenced by rockfill strength and foundation characteristics. The published ranges (Sherard & Cooke, 1987; Jiang & Cao, 1993) coincide with the internal settlements in the cases of CFRDs

Downloaded by [UNIV OF ILLINOIS] on [05/02/20]. Copyright © ICE Publishing, all rights reserved.

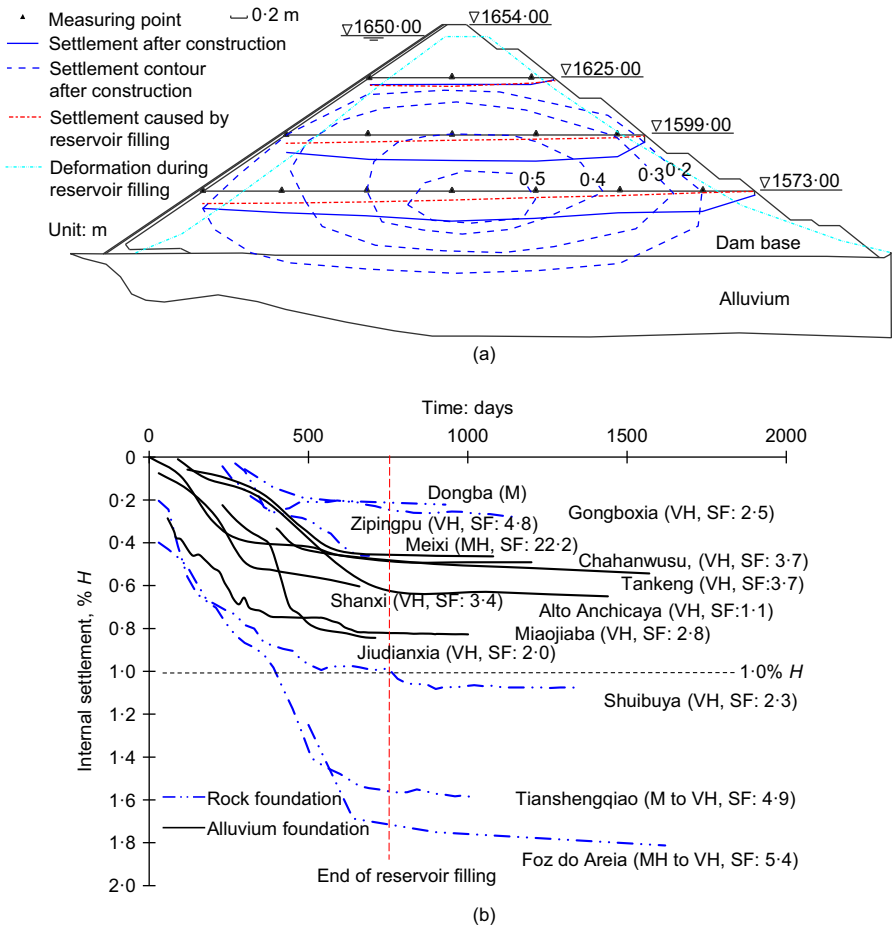

Fig. 7. (a) Distribution of observed internal settlement for the Chahanwusu Dam at the end of its construction. (b) Evolution of the maximum internal settlement of 13 cases with time

built on rock foundation and using VH-strength rockfill to a certain extent. However, the trend considerably underestimates the internal settlements in the cases of CFRDs built on alluvium foundation or using M-strength to MH-strength rockfill.

Several suggested empirical relationships are obtained by regression analysis for several groups of rockfill strengths and foundation conditions in Fig. 8(a). Table 4 presents the suggested empirical relationships for internal settlement. The coefficients of determination (R^2) between measured data and data from suggested relationships are greater than 0·65. The regression coefficients indicate that a good correlation exists for the considered groups. The factors incorporated into the deformation prediction include rockfill strength, foundation conditions and dam height. Dams constructed using VH-strength rockfill and built on rock foundation present a relatively slight increase in internal settlement with dam height. On the contrary, dams constructed using weak rockfill or built on alluvium foundation exhibit a significant increase in internal settlement with dam height. Hunter & Fell (2003) suggested that the internal settlement of a dam on a rock foundation during construction can be estimated using $s = \gamma D H_i / E_v$ (equation (1)). On the basis of database analysis of 35 CFRDs with good-quality monitoring records and construction material data, they established a relationship for estimating the vertical deformation modulus on the basis of the D_{80} size (size for which 80% is fine) and rockfill strength. However, this method ignores the influence of void ratio. Most of the cases presented in Table 1 lack reliable data on vertical deformation modulus. The vertical deformation modulus is only available in 38 cases. Fig. 8(b) presents the relationships between vertical deformation modulus and void ratio considering different rockfill strengths for the 38 cases. A low void ratio and a strong rock result in a high deformation modulus and thus a small internal settlement. Fig. 8(b) provides a modified method for estimating vertical modulus. Fig. 9 compares the predicted internal settlement of eight case histories using the aforementioned prediction methods with the measured values. These cases are selected from Hunter (2003) and are not part of the data used in regression analysis. The calculated mean and standard deviation of error for each method are 0·11 and 0·08 (method suggested by Hunter & Fell), 0·076 and 0·023 (modified vertical modulus estimation method) and 0·054 and 0·015 (suggested relationships in Table 4). The root-mean-square error values for these methods are 0·089, 0·076 and 0·027. The error values of the suggested relationships and modified vertical modulus estimation method are relatively small. These results indicate that the equations by regression analysis in Table 4 and Fig. 8 provide alternative methods for estimating internal settlement and vertical modulus.

Effect of alluvium foundation

Internal settlement behaviour of a dam on an alluvium foundation is analysed. Fig. 10(a) shows the ground settlement of the 14 collected cases with respect to alluvium thickness. Nearly all of the normalised alluvium deformations are less than 1·0% T. Alluvium deformation increases with alluvium thickness and with the decrease in alluvium deformation modulus. The Pappadai Dam exhibits

Downloaded by [UNIV OF ILLINOIS] on [05/02/20]. Copyright © ICE Publishing, all rights reserved.

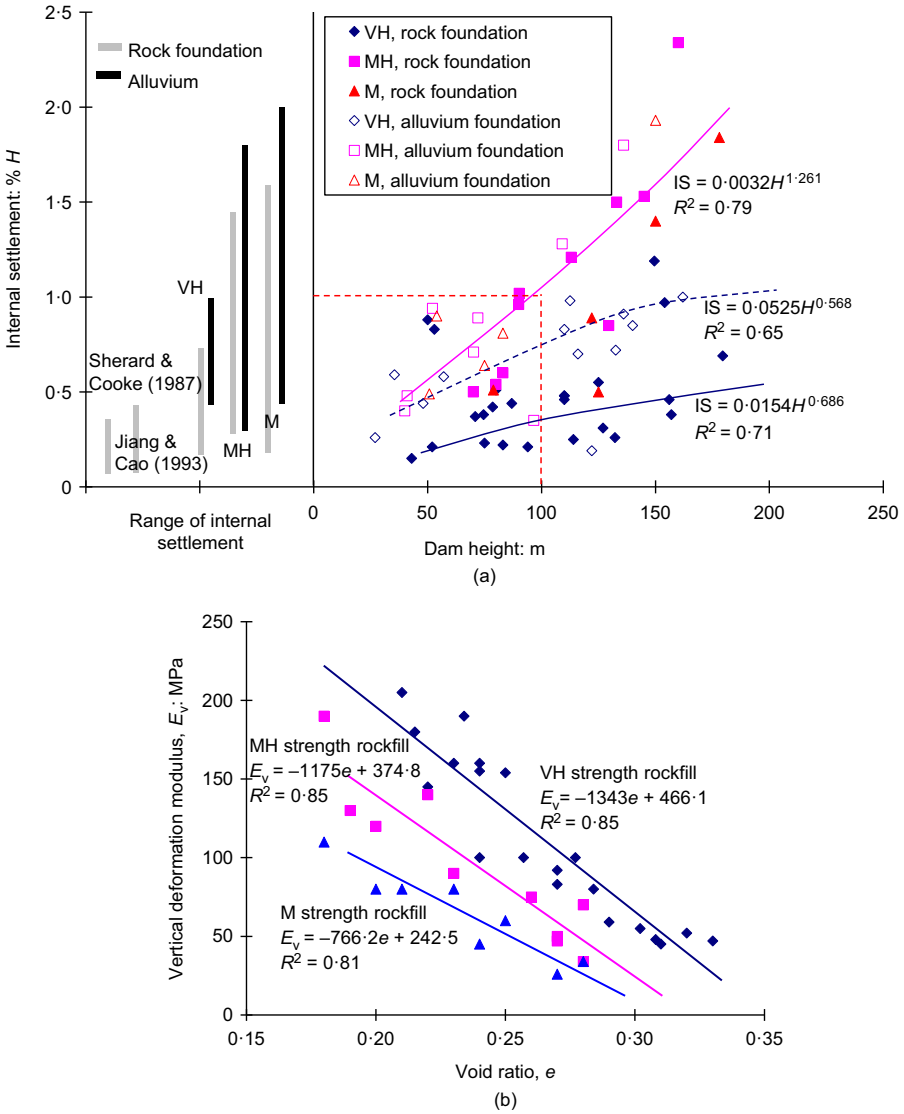

Fig. 8. (a) Internal settlement during construction with respect to dam height. (b) Relationship between void ratio and vertical deformation modulus based on 38 cases

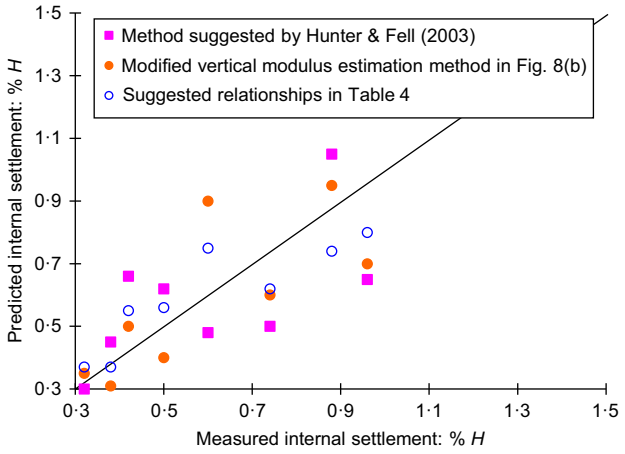

Fig. 9. Comparison of the predicted internal settlement of eight cases adopting prediction methods with the measured values

a small foundation deformation mainly due to its large alluvium deformation modulus and low dam height (27 m only). Fig. 10(b) shows a generalised relationship between dam height and internal settlements along the vertical measuring line of several typical dams, as well as the relationship between the location of maximum internal settlement and relative thickness of the alluvium foundation (T/H) at the end of dam construction based on 11 cases with reliable data.

Under the effect of ground settlement, the maximum internal settlement of CFRDs built on an alluvium foundation occurs at a position of 0·2–0·4H, which is lower than the location of CFRDs built on a rock foundation with a range of 0·4–0·6H. Notably, the location of maximum internal settlement moves downward with the increase in relative thickness of the alluvium foundation and eventually comes close to 0·2H when relative thickness is 0·5. Wen *et al.* (2017) found that foundation compressibility, creep and the hydro-mechanical coupling process are the main mechanisms that result in large dam deformation; among them, foundation compressibility is the main contributing factor.

The internal settlements for 19 cases of CFRDs built on an alluvium foundation are investigated to analyse the effect of the alluvium foundation on dam settlement. These cases are built on an alluvium foundation and have reliable data regarding alluvium thickness and internal settlement. Fig. 11 presents the internal settlements measured at these CFRDs with respect to the relative thickness of the alluvium foundation (T/H). The results show that internal settlements

Downloaded by [UNIV OF ILLINOIS] on [05/02/20]. Copyright © ICE Publishing, all rights reserved.

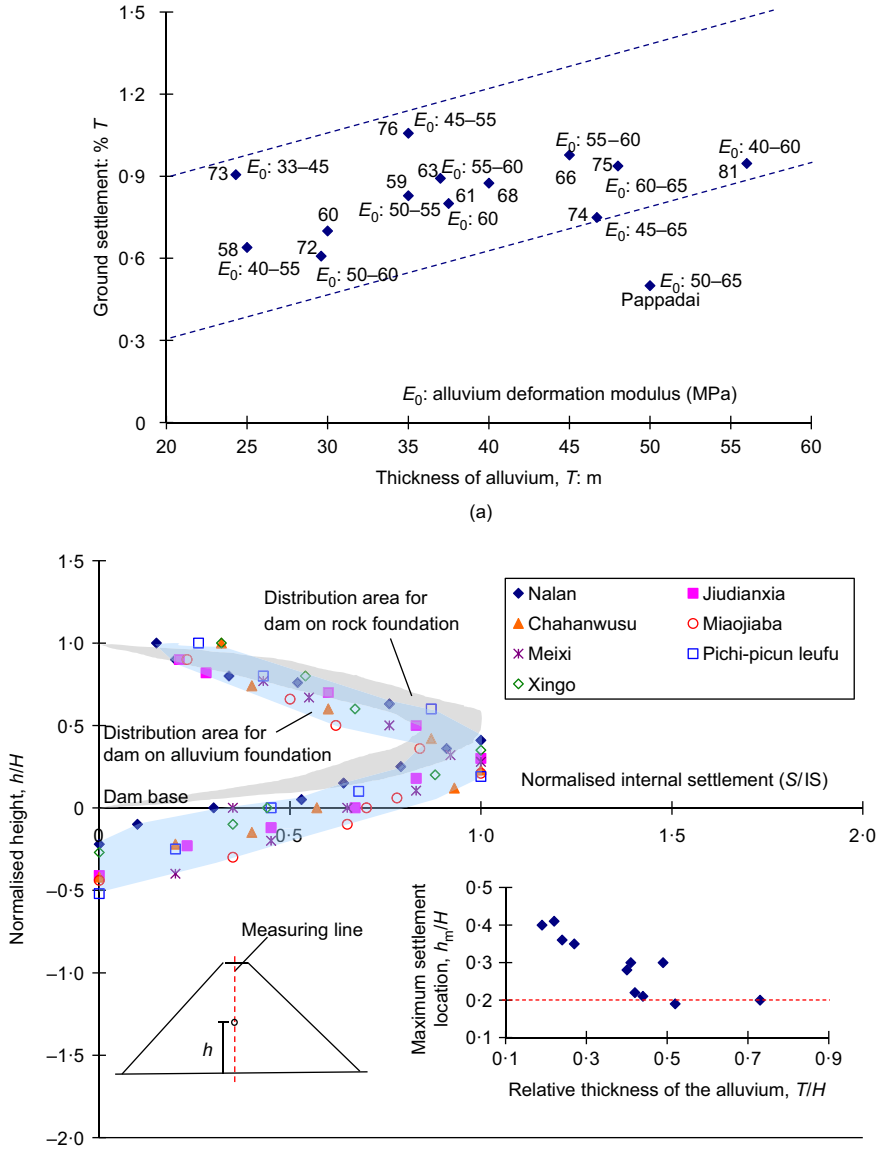

Fig. 10. (a) Ground settlement during construction with respect to alluvium thickness. (b) Relationship between dam height and normalised internal settlement along the vertical measuring line and between the location of maximum settlement and relative thickness of alluvium foundation (T/H) at the end of dam construction. h, height of the measuring point as shown in Fig. 10(b); h_m, height of the measuring point for the maximum internal settlement; S, settlement at the measuring point

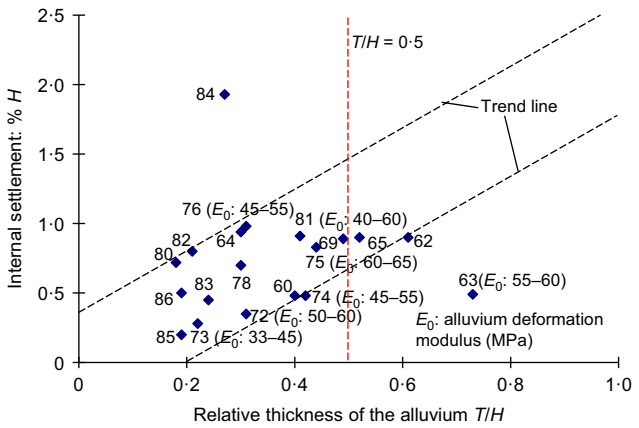

Fig. 11. Internal settlement with respect to the ratio of alluvium thickness and dam height

increase with the relative thickness of the alluvium foundation, with a slope of 0·6 for both trend lines. However, internal settlements do not increase when the relative thickness is greater than 0·5. High T/H ratios mean that the alluvium thickness is large, and is even comparable to the dam height and bottom width. For high T/H ratio, additional stresses in the alluvium layer decrease, whereas ground modulus increases with depth. Reduced additional stress and increased ground modulus may cause small deformation of the alluvium below $0{\cdot}5H$ depth, which exerts a limited effect on the dam deformation. This condition may be the main reason why internal settlements no longer increase with a certain T/H value (0·5) and above. The difference in settlements in Fig. 11 is attributed mainly to rockfill strength, rockfill gradation, valley shape and alluvium deformation modulus. The results show that internal settlements are large when the alluvium deformation modulus is low with similar relative thickness. Xingo Dam and Dahe Dam stand out as outliers to the general trend lines; this may be attributable to the high alluvium modulus and good zone design and compaction of the Dahe Dam (case 63) and the low rockfill

Downloaded by [UNIV OF ILLINOIS] on [05/02/20]. Copyright © ICE Publishing, all rights reserved.

strength, high dam height and wide valley of the Xingo Dam (case 84). These results indicate that the relative thickness and compressibility of an alluvium foundation significantly affect internal settlement.

Effect of valley shape

Figure 12(a) presents the observed internal settlements of case histories during construction with respect to the valley shape factor. A shape factor equal to or smaller than 3 is an indication of a narrow valley (Icold, 2004). When the valley shape factor is less than 3, internal settlement is small but varies significantly. When the valley shape factor is greater than 3, internal settlement is large but varies slightly in a gradual manner. The internal settlement increments after reservoir filling decrease with the increase in the shape factor. The data in Figs 3(a) and 7(b) show that the crest settlement and internal settlement increments after reservoir filling of dams with a shape factor greater than 3 are within 10% of the total deformation. However, the internal settlement increments of dams with a shape factor smaller than 3 are more than 10% and 12% of the total deformation on average and vary significantly. The measured dam deformations in narrow valleys ($SF < 3$) are relatively small in the early years and then increase for many years at a decreasing rate. These results indicate that a cross-valley arching effect is significant for narrow valleys with a shape factor smaller than 3. In narrow valleys, the abutments hinder the settlement of the dam body and result in the arching effect. The arching effect of rockfill reduces the vertical load in the dam section because part of the load is transferred to the abutments, thereby resulting in a lower degree of settlement (Qu *et al.*, 2009).

Figure 12(b) shows that the observed vertical stresses of the dam body at the end of dam construction for two typical dams of similar height in narrow valleys are smaller than the calculated overburden total stresses (rockfill layer thickness multiplied by the unit weight of rockfill). Maximum stress occurs at the bottom of the dam, and the arching effect is significant at the lower central section of the dam. The reduction in vertical stress reaches 40% at measuring point K3 of the Cethana Dam built on rock foundation; this value is significantly larger than 14·5% at a similar location (M4) of the Miaojiaba Dam built on alluvium foundation. Hunter & Fell (2003) reported that, when river width is less than 30–40% H and steep abutment slopes are greater than 50°, the arching effect results in a reduction of more than 20% in vertical stress.

BEHAVIOUR OF FACE SLAB

Face slab deflection pattern

Face slab deflection depends mainly on the deformation of the neighbouring rockfill. Face slab settles and moves towards the downstream under water load. Fig. 13(a) shows the evolution of the maximum face slab deflection of ten cases with time. These cases possess reliable and complete face slab deflection information. Similarly to the internal settlement, the time at the end of reservoir filling of each case is set as the reference time. Face slab deflection increases rapidly during reservoir filling, indicating that the water load significantly affects face slab deflection. The average

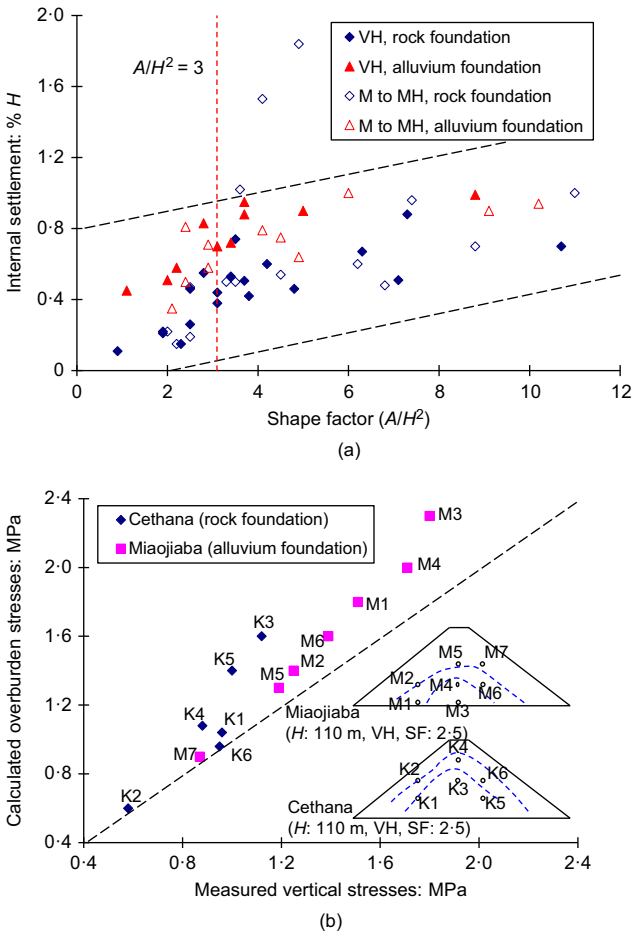

Fig. 12. (a) Internal settlements during construction with respect to the valley shape factor. (b) Measured vertical stresses plotted against calculated total overburden stresses at the end of dam construction at the maximum cross-section of two typical dams

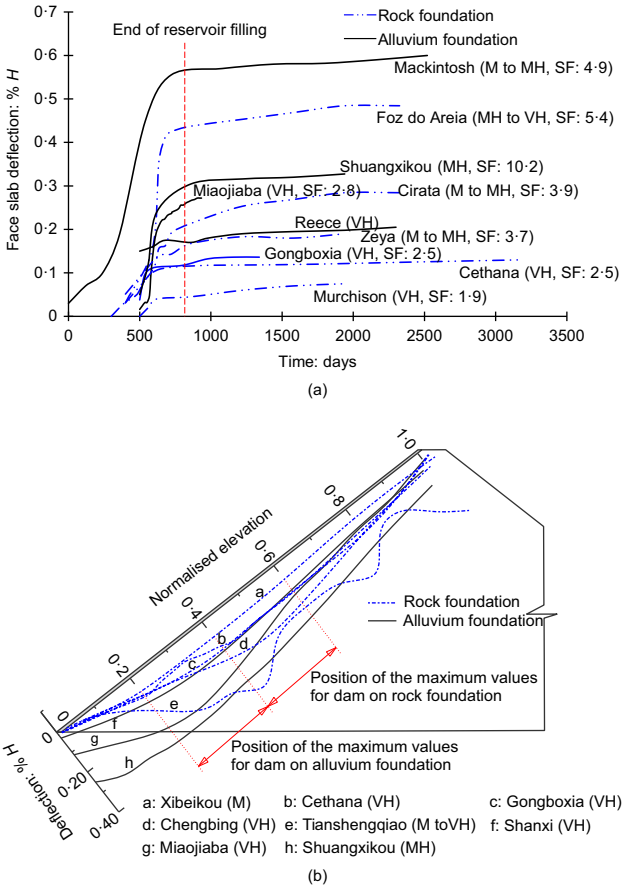

Fig. 13. (a) Evolution of the maximum face slab deflection of ten cases with time. (b) Normalised face slab deflection distributions after reservoir filling at typical sections of eight cases

Downloaded by [UNIV OF ILLINOIS] on [05/02/20]. Copyright © ICE Publishing, all rights reserved.

deformation rate is smaller than 2 mm/year after reservoir filling. This finding coincides with the report of Fitzpatrick *et al*. (1985), who presented that the average deformation rate during the first 10 years after impoundment is approximately 3 mm/year. Similarly to dam settlement, large face slab deflections are observed for dams built on alluvium and constructed using low-strength rockfill. Fig. 3(b) shows that approximately 80% of the total face slab deflection occurs during reservoir filling for CFRDs built on an alluvium foundation; this value is larger than 74% for dams on a rock foundation. Water load exerts a significant effect on the deflection of dams constructed using low-strength rockfill. The effect of reservoir filling on face slab deflection is more significant than that of reservoir filling on crest settlement.

Figure 13(b) shows the measured deflection distributions after reservoir filling at typical sections of eight cases. From the measured deflection distributions, the deflection patterns can be characterised as a D-shape distribution with maximum deflection close to 0·2–0·6 dam height from the dam base (e.g. the Chengbing Dam and Miaojiaba Dam). Occasionally, a B-shape distribution is observed to exhibit a large face slab deflection near the upper and centre parts (e.g. the Tianshengqiao Dam). Figure 13(b) shows that, under the effect of foundation deformation, the maximum face slab deflections of dams built on an alluvium foundation are generally larger than those of dams built on a rock foundation; their position (0·2–0·4H) moves down.

Statistical analysis on face slab deflection

Figure 14 presents the face slab deflection measured in the 87 case histories with respect to dam height for different rockfill strengths and foundation characteristics. Most cases exhibit face slab deflection values of less than 0·40% H, and more than half exhibits values of less than 0·2% H. However, the Mackintosh Dam (0·65% H), Jiudianxia Dam (0·62% H) and Tianshengqiao Dam (0·64% H) exhibit large face slab deflection values. Such large values may be attributed to the large alluvium foundation thickness (56 m) of the Jiudianxia Dam, the large height (178 m) of the Tianshengqiao Dam and the low rockfill modulus (30 MPa) of the Mackintosh Dam. Table 3 and Fig. 14 show that face slab deflection is slightly larger at dams with a measuring period of more than 5 years than that for a period of less than 5 years; however, the difference is not marked. This observation is because most face slab deformations occur during the first reservoir filling. Similarly to dam settlement, large face slab deflections are observed for CFRDs built on an alluvium foundation or constructed using low-strength rockfill. The difference in the upper range of the face slab

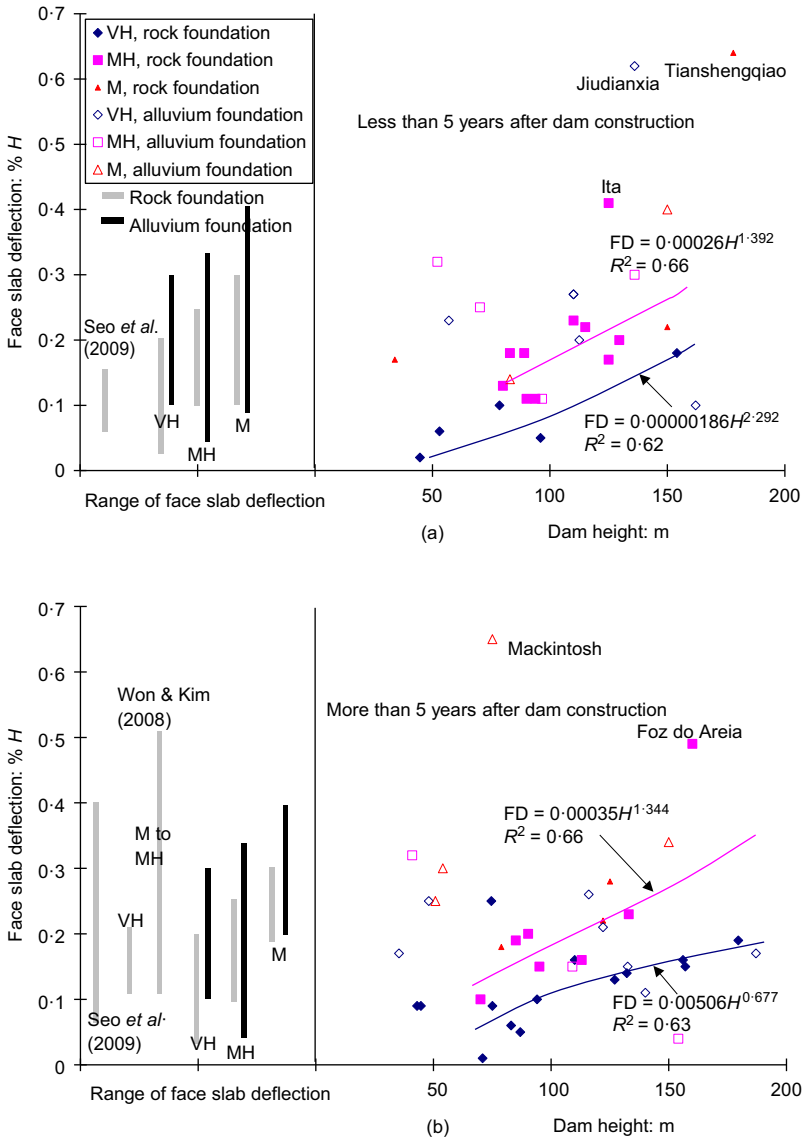

Fig. 14. Face slab deflection with respect to dam height in: (a) less than 5 years; (b) more than 5 years

Downloaded by [UNIV OF ILLINOIS] on [05/02/20]. Copyright © ICE Publishing, all rights reserved.

deflection between dams on a rock or alluvium foundation constructed using VH-strength rockfill and M-strength rockfill is approximately 0·1% H. The face slab deflection of dams on an alluvium foundation is 0·08% H greater than that of dams on a rock foundation. The difference in the upper range is approximately 0·1% H, which indicates that face slab behaviour is significantly affected by foundation characteristics and rockfill strength. Fig. 14 shows that the published ranges (Won & Kim, 2008; Seo *et al.*, 2009) underestimate the face slab deflection in the cases of dams with a measuring period of less than 5 years but overestimate that of dams with a period of more than 5 years.

Pinto & Marques (1998) developed an empirical relationship to estimate the maximum face slab deflection during reservoir filling on the basis of the measured deformations. Face slab deflection is proportionate to H^2/E_v, and the proportionality increases with A/H^2. However, this method may be prone to major errors owing to the same factors that lead to major errors for the empirical prediction of crest settlement. Hunter & Fell (2003) used equation (2) to estimate face slab deflection caused by reservoir filling. E_t is estimated from the E_t/E_v ratio determined by dam height and upstream slope angle, where E_v is estimated from the D_{80} size and UCS of rockfill. This method obtains an approximate result and is only applicable for CFRDs with simple zoning. Several suggested empirical relationships are obtained by regression analysis for dams built on rock foundation and constructed using VH-strength or MH-strength rockfills in Fig. 14. Outliers to the general trend (the Ita Dam and the Foz do Areia Dam) are excluded from the correlations. The evolution of face slab deflection with dam height is non-linear. The suggested empirical relationships between face slab deflection and dam height in the form of a power function are summarised in Table 4. The regression coefficients indicate that a good correlation exists for the considered groups. Similarly to crest settlement, the factors incorporated into the deformation prediction include measuring period, rockfill strength, foundation conditions and dam height. The suggested empirical relationships are derived from a good-quality data set and consideration of the significant factors and are thus alternative methods for estimating face slab deflection.

Figure 15 shows that face slab deflection is very close to crest settlement. More than 80% of the data points fall within the bounds shown in the plot. However, the Jiudianxia Dam exhibits large face slab deflection probably because of its thick alluvium (56 m), and the Wananxi Dam and Xingo Dam present large crest settlement, possibly owing to their complex zoning and low-strength rockfill. Further analysis reveals that the face slab deflections of CFRDs built on alluvium foundation or constructed using low-strength rockfill are slightly larger than the crest settlements; however, the difference does not exceed 0·1% H. The average face slab deflection is 1·1 times the crest settlement. The large face slab deflection may be caused by a large internal settlement. Similarly, Fitzpatrick *et al.* (1985) found that face slab deflections are generally 60% of crest settlements. Won & Kim (2008) and Seo *et al.* (2009) reported that crest settlement and face slab deflection are generally similar, but crest settlement is smaller than face slab deflection when dam height is more than 100 m.

Stress in the face slab

Previous stress observations for typical dams (Arici, 2013; Mahabad *et al.*, 2014; Wang *et al.*, 2014) have demonstrated that most slope-direction stresses (in the direction parallel to the slope) under water load are compressive, except near the toe, the crest and the abutments on both sides of the face slab where stresses are tensile. Moreover, the maximum tensile stress always occurs at the bottom of the face slab. Fig. 16 shows the measured slope-direction stresses in the face slab of seven typical CFRDs after reservoir filling. The maximum compressive stresses (1·0–16·5 MPa) occur near the bottom, whereas some tensile stresses are observed near the toe and the top. The observed compressive stresses are within the acceptable range. The maximum tensile stresses near the bottom of the Cethana Dam and the crest of Tianshengqiao Dam reach 2·0 and 1·5 MPa, respectively. These tensile stresses exceed the tensile strength of the concrete. A group of tensile cracks is observed near the bottom of the Cethana Dam (Fitzpatrick *et al.*, 1985) and the crest of the Tianshengqiao Dam (Zhang *et al.*, 2004), and most of them are oriented horizontally.

The behaviour of a CFRD built on an alluvium foundation is investigated using the three-dimensional (3D) finite-element deformation analysis of the Miaojiaba Dam by Wen *et al.* (2017). The behaviour of rockfill and alluvium is described using an elasto-plasticity model (Zhang *et al.*, 2007), which can capture volumetric strain behaviour. A creep model (Zhou *et al.*, 2011) is used to obtain a time-dependent deformation. The computational parameters are deduced from triaxial tests and back-analysis. The concrete-face slab is simulated using a linear elastic model.

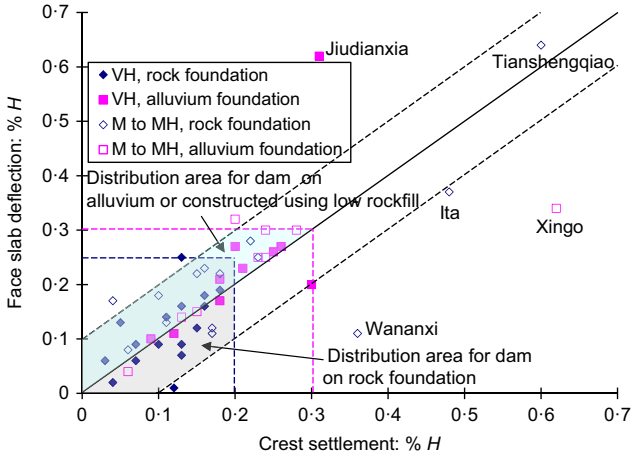

Fig. 15. Comparison of face slab deflections and crest settlements of all cases

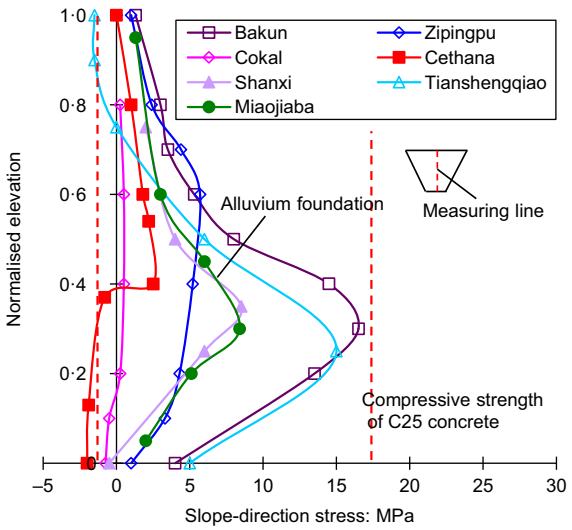

Fig. 16. Measured slope-direction stresses in the downstream face of the face slab of seven CFRDs after reservoir filling

Downloaded by [UNIV OF ILLINOIS] on [05/02/20]. Copyright © ICE Publishing, all rights reserved.

The behaviour of the concrete–fill interface is modelled using a friction contact method, which considers the rockfill and the face slab as two independent deformation bodies that follow the Coulomb friction law at the contact interface when they contact each other (Zhang *et al*., 2004). Five rows of elements are divided in the thickness direction of the face slab to reflect the behaviour accurately. A total of 1650 spatial eight-node isoparametric elements are used for the face slab. The computational procedure follows the construction and subsequent reservoir-filling processes, where the construction of the face slab is simulated in three stages. Fig. 17 shows the distribution of slope-direction stress in the upstream of the face slab after reservoir filling based on the 3D numerical simulation by Wen *et al*. (2017). Most face slab parts are under compression because of their own weight at the end of construction. During reservoir filling, water pressure increases the shear transfer between the face slab and the underlying rockfill; consequently, compressive and tensile stresses occur in the central parts of the face slab and in the perimeter areas, respectively. The maximum tensile stress of 1·10 MPa occurs at the corner of the face slab. The distribution of horizontal stress (in the direction along the dam axis) is similar to that of the slope-direction stress. These results are consistent with the observations for typical dams.

The tensile stress in the face slab is caused by two main mechanisms: (*a*) face slab deflection or a bulging deformation of the dam body causing a large moment in the side and the bottom, thereby inducing tensile stresses; (*b*) large movement of rockfill dragging the face slab towards the centre and causing significant tensile forces at the border, thereby inducing additional tensile stresses. Fig. 17 shows the deformation trend of the face slab and moment and axial force distribution in the middle part of the face slab after reservoir filling. Water pressure during reservoir filling increases shear resistance, thereby facilitating tensile zones and always causing maximum tensile stresses at the bottom. Mahabad *et al*. (2014) asserted that the development of the tensile stresses in the face slab and their increase with depth are consistent with the increase in the shear resistance between the face slab and neighbouring dam body. Cushion zone stiffness, extruded curb and vertical joints significantly affect the tensile stress of the face slab (Zhang & Zhang, 2009; Mahabad *et al*., 2014).

Separation and cracking of face slab

The face slab in a CFRD typically serves as the only barrier to seepage through the dam. Excessive deformation of rockfill causes separation between the face slab and cushion layer or even cracks in the slab (Modares & Quiroz, 2016). Severe cracking can result in excessive leakage and lead to further damage to the face slab. Therefore, the face slab must be designed with cracking resistance. The mechanism of separation and cracking of face slab is explored. Table 5 presents the separation deformation and cracking of face slab for 11 in-service CFRDs.

The observed separation between the face slab and cushion occurs mainly during construction and is caused by different deformations between the face slab and the rockfill. During construction, separation occurs mainly in the upper zone of slabs at different stages, and the maximum opening occurs in the middle part. Fig. 18 shows the typical separation deformation and distribution during construction. Zhang *et al*. (2004) reported that post-construction creep deformation of rockfill enlarges the separation on upper face slabs. With reservoir filling, the face slab and cushion layer come into contact again because of water pressure, thereby drastically decreasing the separation (Zhang & Zhang, 2009). Only limited monitoring data relating to separation deformation are included because of the difficulties in obtaining reliable data. Therefore, the aforementioned conclusions cannot be further verified by the monitoring data in this study.

Concrete-face rockfill dams are affected mainly by the cracking of face slab, which causes leakage and reduces safety factors. The observed cracking indicates that the mechanisms which cause cracking in face slabs include: (*a*) rockfill deformation caused by reservoir filling and rockfill creep; (*b*) thermal cracking; and (*c*) shrinkage cracking. The extrusion damage and cracks (structural cracks) caused by structure-induced stress produced by dam gravity, water pressure and rockfill creep are the key issues for face slab. Large rockfill deformation is the major cause of these cracks. Structural cracks are a result of tensile failure or shear failure, which are initiated where tensile stresses exceed the tensile strength of concrete materials. Most observed structural cracks are located in the bottom and at both sides, as the structure-induced tensile stress occurs mainly in the perimeter areas of face slab, as analysed previously. Under the effect of face slab moment and the dragging effect of the dam body, the principal tensile stress is in the direction parallel to the slope at the top and bottom of the face slab. This phenomenon leads to the development of horizontal cracks. At both sides, the face slab suffers more horizontal tensile stress than slope-direction stress as a result of the dragging effect of the dam body. In addition, the uneven deformation of rockfill at the abutment causes shear failure in the face slab. The combined effect of horizontal tensile

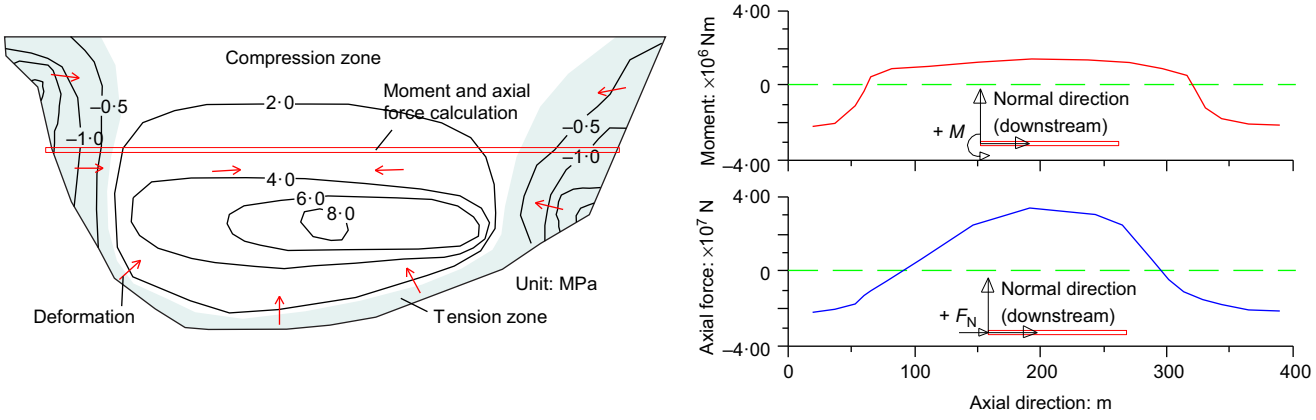

Fig. 17. Slope-direction stress distribution in the downstream of the face slab and moment and axial force distribution in the middle part of the face slab for the Miaojiaba Dam after reservoir filling

Downloaded by [UNIV OF ILLINOIS] on [05/02/20]. Copyright © ICE Publishing, all rights reserved.

Table 5. Summary of separation deformation and cracking of face slab for 11 CFRDs

Dam	*H*: m	Face slab area: $\times 10^3$ m^2	Separation during construction	Cracking of face slab			
				Cracking	Position	Construction stage	Cause
Aguamilpa	187	136·4	—	Cracks parallel to the plinth	Right bank	After face slab placement	Rockfill deformation
Gongboxia	132·2	0·8	10 cm (width), 5·1 m (depth)	Vertical crack	Top	Operation period	Temperature-induced stress and rockfill deformation
Ita	125	6·1	12 cm (width), 6·5 m (depth)	Horizontal cracking	Bottom	During reservoir filling	Foundation geometry
Lesu	60	—	—	Slabs cracking	Right abutment	Operation period	Rockfill creep
Shuibuya	233	124·9	23 cm (width), 7·5 m (depth)	Horizontal cracking	Top and bottom	During reservoir filling	Improper construction schedule of slabs and rockfill deformation
Tianshengqiao	178	103·9	15 cm (width), 6·8 m (depth)	Horizontal cracking	Bottom	During reservoir filling	Dam body construction sequence
Xibeikou	95	1·0	6 cm (width), 2·3 m (depth)	Horizontal cracking	Front panel	During construction	Temperature-induced stress and shrinkage stress
Xingo	150	135	—	Cracks parallel to the plinth	Right bank	During reservoir filling	Rockfill uneven deformation
Mohale	145	110	—	Extrusion damage	Central part	During reservoir filling	Rockfill deformation
Barra Grande	185	120	—	Extrusion damage	Central part	After reservoir filling	Water pressure
Campos Novos	202	55	—	Extrusion damage	Central part	During reservoir filling	Rockfill deformation

stress and potential shear failure may be the cause of cracks at both sides parallel to the plinth. Vertical cracks owing to extrusion failures are also observed in the central part of the face slab in some CFRDs. Large rockfill deformation causes an extrusion effect at the vertical joints of the central face slab. The extrusion effect causes large horizontal compressive stress and significant stress concentration that result in extrusion failures. Vertical cracks because of extrusion failure occur mainly in dams with a height of more than 150 m. The typical distribution pattern of cracking during reservoir filling is presented in Fig. 18.

The cracking behaviour of face slab changes at different periods. During reservoir filling, water pressure facilitates large face slab deflection and leads to most of the crack developments. In the long term, the extent of the cracked region is significantly reduced as a result of the reduction in tensile stresses caused by the settlement of the rockfill (Arici, 2011). Arici (2011, 2013) examined the cracking behaviour of face slab for the Cokal Dam. Reservoir filling causes tensile cracking at the bottom of the face slab with a maximum crack width of 1·0 mm. Similarly, in the long term, the average crack width is reduced from 0·5 mm to 0·4 mm and the extent of the cracked region is significantly reduced.

LEAKAGE OF CFRDS

Statistical analysis on CFRD leakage

Leakage at a CFRD mainly depends on the working state of the joints of the seepage control system, as well as the presence or absence of cracks and defects in the seepage barriers. Excessive leakage can cause economic loss of water and affect the function of the reservoir. In this section an attempt is made to discuss the statistical law of the leakage of CFRDs with different dam heights. Fig. 19(a) shows the relationship of leakage after reservoir filling of all the cases plotted against dam height.

The leakage rate of dams built on rock foundation is less than 60 l/s when dam height is less than 125 m; however, the leakage rate increases between approximately 60 and 120 l/s when dam height is higher than 125 m. This phenomenon may be attributed to the significant opening of joints and the cracking of seepage barriers for high dams because of water load. Rice & Duncan (2010a, 2010b) and Brown & Bruggemann (2002) found that even small joint openings or cracks with apertures less than a millimetre in the seepage barrier can significantly increase the effective hydraulic conductivity and result in a significant increase in leakage rate. The leakage rate of dams built on alluvium foundation rapidly increases between around 80 and 180 l/s when dam height is more than 125 m. The leakage rate increases exponentially with dam height. A relationship between the leakage rate and dam height is fitted to $L = 0{\cdot}000906H^{2{\cdot}242}$ for dams on rock foundation and $L = 0{\cdot}2017H^{1{\cdot}268}$ for dams on alluvium foundation. The leakage rate of CFRDs built on an alluvium foundation is considerably larger than that of CFRDs built on a rock foundation, especially when dam height is more than 125 m. This result may be attributed to large leakages in the foundation, as well as a large number of cracks or defects in the seepage barriers caused by foundation deformation. Large leakages are recorded in the Alto Anchicaya Dam (140 m), Xingo Dam (150 m) and Aguamilpa Dam (187 m), which are built on an alluvium foundation. These dams present such large leakage mainly because they have experienced significant face slab cracking (Table 5). A leakage of a few tens of litres per second exerts negligible economic value (Cruz *et al.*, 2007). However, CFRDs higher than 125 m may experience some leakage problems. Fig. 19(a) shows a broad range of leakage rates

Downloaded by [UNIV OF ILLINOIS] on [05/02/20]. Copyright © ICE Publishing, all rights reserved.

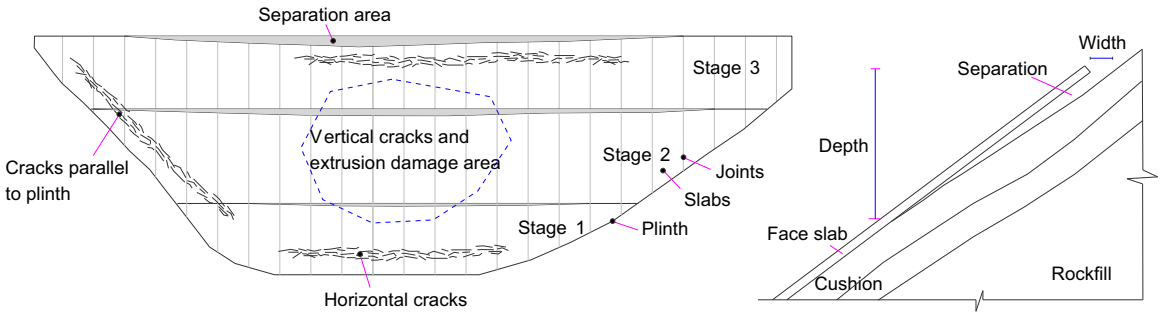

Fig. 18. Typical separation during construction and distribution pattern of cracking during reservoir filling for face slab

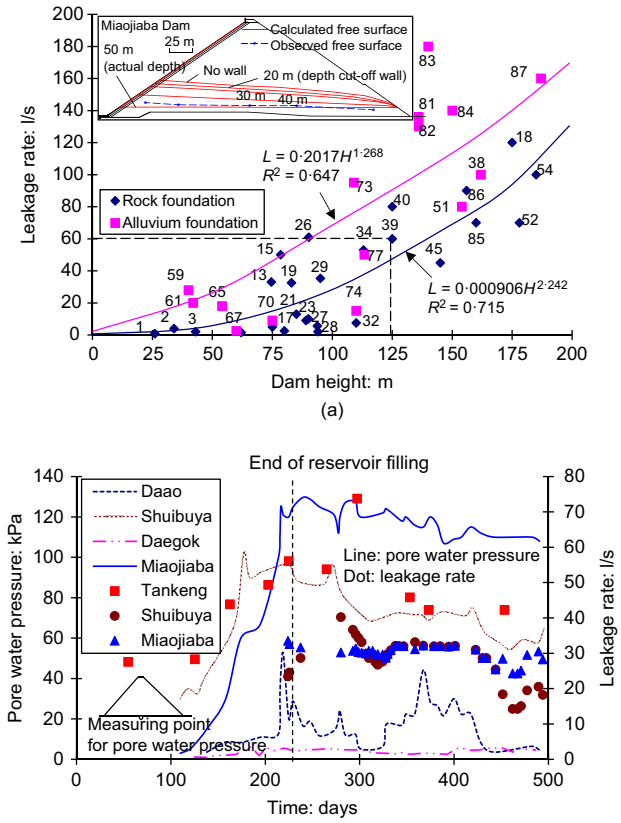

Fig. 19. (a) Leakage after reservoir filling with respect to dam height. (b) Evolutions of measured pore water pressure and leakage rate of several typical CFRDs

within the different foundation characteristics and height groupings. Attempts to incorporate other influencing factors of leakage rate, such as dam length, result in a high degree of data variability. Theoretically, the leakage rate depends on the thickness and length of cracks in seepage barriers and on the water pressure at the location of the cracks. The number of cracks and their locations become important when leakage rate is given for the entire dam, which indicates that dam length is also a key influencing factor of leakage rate. Table 1 shows that leakage rate exhibits a tendency to increase with crest length in the case of similar dam height.

The efficiency of a cut-off wall as a seepage barrier based on case history data has been rarely reported because of the difficulty in assessing leakage in deep, permeable deposits below a CFRD (Brown & Bruggemann, 2002). The leakage rates of most of the CFRDs built on rock or alluvium foundations fall within the acceptable range, especially when dam height is less than 125 m. This finding indicates that the seepage flow of the dam is effectively prevented by the seepage control system. Wen *et al.* (2017) conducted a non-steady saturated seepage flow analysis for the Miaojiaba Dam. A parabolic variational inequality formulation of Signorini's condition was adopted to determine the free surface and seepage points of the saturated seepage process. The results of the non-steady seepage calculation (Fig. 19(a)) show that the seepage in an alluvium foundation is effectively prevented only when the cut-off wall is embedded in bedrock and cuts off the alluvium. The free surface is high and alluvial erosion can occur when a suspended cut-off wall is adopted. This phenomenon is possible due to the increased hydraulic gradients and developed velocities beneath and around the wall or in the openings of the wall (Brown & Bruggemann, 2002; Rice & Duncan, 2010b).

Figure 19(b) plots the evolutions of measured leakage rate and pore water pressure in the foundation under a typical cross-section of several typical CFRDs. The pore water pressure under the dam body is less than 0·15 MPa, which indicates that the free surface in the dam body is very low (not more than 15 m higher than the riverbed) and that nearly no pore water pressure occurs in the rockfill. Pore water pressures increase and fluctuate with reservoir level. At the end of reservoir filling, the pore water pressures reach peak values, decrease mildly and tend to stabilise. The pore water pressure of the Daao Dam fluctuates significantly approximately 150 days after reservoir filling, which may be attributed to the flood factor. Rainfall can also affect pore water pressure. The evolutions of leakage rate are similar to the variations in pore water pressure. The maximum leakage rate is reached immediately after reservoir filling and decreases to a steady state in the long term. This process can be explained by the fact that the extent and width of existing cracks are reduced in the long term (Arici, 2011). In addition, the hydraulic conductivity of the rockfill slightly decreases as a result of the coupling effect of seepage and deformation (Chen *et al.*, 2011; Elia *et al.*, 2011). Furthermore, the filling of joint openings caused by small particles in the cushion can reduce the leakage.

Effect of seepage flow on deformation behaviour

Large quantities of water pass through CFRDs without observations of significant dam settlement caused by seepage flow, as previously reported (Cruz *et al.*, 2007; Battaglia *et al.*, 2016; Jia *et al.*, 2016). Chen *et al.* (2011) concluded that the effect of seepage flow on dam deformation is insignificant on the basis of a coupled hydro-mechanical analysis of the Shuibuya Dam. Freitas & Cruz (2007) found no significant additional dam settlements caused by large leakages during reservoir operation on the basis of previous experiences. These conclusions can be further validated by examining the results in Fig. 20. Thus, cases with a

Downloaded by [UNIV OF ILLINOIS] on [05/02/20]. Copyright © ICE Publishing, all rights reserved.

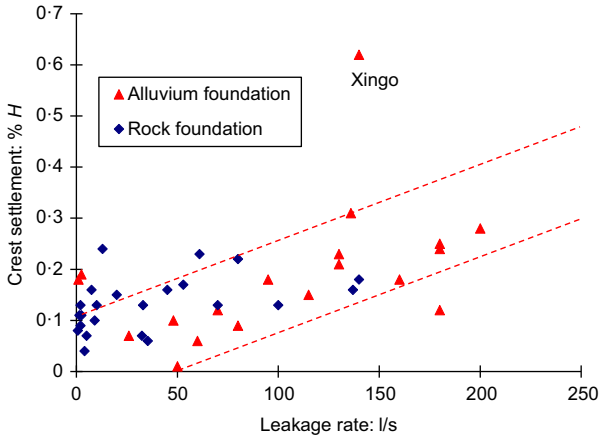

Fig. 20. Relationship of crest settlement plotted against leakage in more than 5 years

measuring period of more than 5 years are selected in the analysis to avoid interference from the measuring period. No significantly large crest settlement for dams is observed with large leakage. Although crest settlement is affected by various factors and broadly varies within different leakage groupings, the results still provide meaningful insights into the effect of leakage on dam behaviour.

These observations are related to a mechanism associated with the granular structure of rockfill. The compacted rockfill possesses a structural skeleton, which carries the weight of the overlying dam. The contact compressive stresses between the rocks comprising the skeleton are high (approaching rock compressive strength) because the contact areas are small. These high compressive stresses create high frictional resistances that are much larger than the drag forces caused by seepage flow through the voids. These results can also be related to the fact that seepage exists only in a few portions of the rockfill. Fig. 20 shows that the crest settlement of CFRDs built on an alluvium foundation increases with leakage; however, the correlation is unclear because seepage flowing through the alluvium may cause foundation erosion, thereby loosening the internal structure of the alluvium and causing some additional crest settlements.

Although seepage exerts a limited effect on dam settlement, the water that penetrates through the face slab can cause significant wetting deformation during reservoir filling. The penetrating water wets the rockfill, such that the additional dam settlement is induced owing to the reduction in bond strength (Xing *et al.*, 2006; Zhou *et al.*, 2011). Collapse settlement can also occur during reservoir filling because of the wetting of rockfill; however, this deformation is significant in earth core rockfill dams (Mahinroosta *et al.*, 2015). In addition, large leakage after reservoir filling can threaten dam stability if the dam does not possess zones of high-permeability rockfill to drain water effectively. CFRDs constructed with sand and gravel or rockfill with a high fine fraction always exhibit limited capability to discharge leaks. The Gouhou Dam in China, which was built with sand and gravel, presents dam stability failures related to seepage flow (Chen & Zhang, 2006).

CONCLUSIONS

This paper reports the statistical results of the deformations and leakage of CFRDs from 87 case histories. Post-construction crest settlement, internal settlement, face slab behaviour and leakage of CFRDs are studied. The effects of rockfill strength, alluvium foundation, valley shape and seepage flow on dam behaviour are discussed. The conclusions of the study are listed below.

(*a*) The behavioural trends of CFRDs are obtained on the basis of statistical analysis conducted on case histories. Most CFRDs exhibit crest settlements of 0·4% H or smaller and exhibit internal settlements of less than 1·0% H during construction. Face slab deflection after reservoir filling is very close to crest settlement, but the face slab deflection of dams built on an alluvium foundation or constructed using low-strength rockfill is slightly larger than the crest settlement. Most face slab deflections are less than 0·40% H, and more than half of them exhibit values of less than 0·2% H. Large rockfill deformations are major causes of tensile stresses as well as cracking and extrusion damage in the face slab. The expected behavioural trends are obtained; the findings offer reliable insights into dam behaviour and provide engineering analogy and reference for the design and construction of CFRDs.

(*b*) The suggested empirical relationship is considered to provide a reasonable basis for estimating the deformation and seepage behaviour of CFRDs on the basis of the statistics of case histories because extensive data are studied and additional factors that influence dam behaviour are considered. An artificial neural network model is also an alternative method for predicting CFRD behaviour.

(*c*) The deformation behaviour of CFRDs is affected by foundation characteristics, intact rock strength, valley shape and seepage flow. Rockfill strength and foundation characteristics are the main influencing factors of dam deformation behaviour. Large dam settlements are observed for CFRDs built on an alluvium foundation or constructed using low-strength rockfill. These dams need much time to reach a small settlement rate. The location of maximum internal settlement moves downwards with the increase in the relative thickness of the alluvium foundation (T/H) and eventually comes close to 0·2H when the relative thickness is 0·5. The first reservoir filling significantly affects dam behaviour, especially face slab deflection. The arching effect is significant when the valley shape factor is less than 3. The effect of seepage flow on dam deformation is insignificant.

(*d*) The maximum values of pore water pressure and leakage occur immediately after reservoir filling and decrease to a steady state in the long term. CFRDs higher than 125 m may experience a few problems with leakage, especially when these dams are built on an alluvium foundation because of the opening of joints and the cracking of seepage barriers.

ACKNOWLEDGEMENTS

This study was supported by the National Natural Science Foundation of China (51722907, 51679197, 51579207 and 51679193).

NOTATION

A	upstream slope face area
a, b, c	coefficient of the empirical prediction methods
D	settlement layer thickness
d	height of inclined column normal to face slab
E_t	transverse modulus of deformation
E_v	vertical modulus of deformation
E_0	alluvium deformation modulus

Downloaded by [UNIV OF ILLINOIS] on [05/02/20]. Copyright © ICE Publishing, all rights reserved.

e void ratio
H dam height
H_i thickness of the dam body above the considered layer
h, h_m height of the measuring point
h_i depth from the reservoir surface
L leakage rate after reservoir filling
R^2 coefficient of determination
S settlement at the measuring point
S, D, H_i relevant variables for defining E_v
s settlement of the considered layer
T alluvium thickness
t_1, t_2 time in month
γ unit weight of rockfill
γ_w unit weight of water
δ_s, h_i, d relevant variables for defining E_t

REFERENCES

Arici, Y. (2011). Investigation of the cracking of CFRD face plates. *Comput. Geotech.* **38**, No. 7, 905–916.

Arici, Y. (2013). Behaviour of the reinforced concrete face slabs of concrete faced rockfill dams during impounding. *Struct. Infrastruct. Engng* **9**, No. 9, 877–890.

Battaglia, D., Birindelli, F., Rinaldi, M., Vettraino, E. & Bezzi, A. (2016). Fluorescent tracer tests for detection of dam leakages: the case of the Bumbuna dam – Sierra Leone. *Engng Geol.* **205**, 30–39.

Brown, A. J. & Bruggemann, D. A. (2002). Arminou Dam, Cyprus, and construction joints in diaphragm cut-off walls. *Géotechnique* **52**, No. 1, 3–13, https://doi.org/10.1680/geot.2002.52.1.3.

Charles, J. A. (2008). The engineering behaviour of fill materials: the use, misuse and disuse of case histories. *Géotechnique* **58**, No. 7, 541–570, http://dx.doi.org/10.1680/geot.2008.58.7.541.

Chen, Q. & Zhang, L. M. (2006). Three-dimensional analysis of water infiltration into the Gouhou rockfill dam using saturated–unsaturated seepage theory. *Can. Geotech. J.* **43**, No. 5, 449–461.

Chen, Y., Hu, R., Lu, W., Li, D. & Zhou, C. (2011). Modeling coupled processes of non-steady seepage flow and non-linear deformation for a concrete-faced rockfill dam. *Comput. Structs* **89**, No. 13–14, 1333–1351.

Clements, R. P. (1984). Post-construction deformation of rockfill dams. *J. Geotech. Engng* **110**, No. 7, 821–840.

Cooke, J. B. (1984). Progress in rockfill dams. *J. Geotech. Engng* **110**, No. 10, 1381–1414.

Cooke, J. B. & Sherard, J. L. (1987). Concrete-face rockfill dam: II. design. *J. Geotech. Engng* **113**, No. 10, 1113–1132.

Cruz, P. T., Freitas, J. & Monoel, S. (2007). Cracks and flows in concrete face rockfill dams (CFRDs). *Proceedings of symposium on dam engineering*, Lisbon, Portugal, pp. 1–14.

CSHE (China Society for Hydropower Engineering) (2007). *Practice and development of building dam with overburden. China hydropower engineering society of hydraulic and hydropower station buildings professional committee*. Beijing, China: China Water Conservancy and Hydropower Press.

Dolezalova, M. & Hladik, I. (2011). Constitutive models for simulation of field performance of dams. *Int. J. Geomech.* **11**, No. 6, 477–489.

Dounias, G. T., Kountouris, A. & Anastasopoulos, K. (2012). Long-term behaviour of embankment dams: seven Greek dams. *Proc. Instn Civ. Engrs – Geotech. Engng* **165**, No. 3, 157–177, http://dx.doi.org/10.1680/geng.11.00052.

Elia, G., Amorosi, A., Chan, A. H. C. & Kavvadas, M. J. (2011). Fully coupled dynamic analysis of an earth dam. *Géotechnique* **61**, No. 7, 549–563, https://doi.org/10.1680/geot.8.P.028.

Fell, R., Macgregor, P., Stapledon, D. & Bell, G. (2005). *Geotechnical engineering of dams.* London, UK: Balkema/Taylor & Francis.

Fitzpatrick, M. D., Cole, B. A., Kinstler, F. L. & Knoop, B. P. (1985). Design of concrete-faced rockfill dams. In *Concrete face rockfill dams: design, construction and performance*, (eds J. B. Cooke and J. L. Sherard), pp. 410–434. New York, NY, USA: American Society of Civil Engineers.

Freitas, M. S. & Cruz, P. T. (2007). Unpredicted cracks and ruptures at face slab in CFRDs – repairing works and treatment. *Proceedings of the workshop on high dam know-how*, Yichang, China, pp. 75–90.

Gan, L., Shen, Z. Z. & Xu, L. Q. (2014). Long-term deformation analysis of the Jiudianxia concrete-faced rockfill dam. *Arabian J. Sci. Engng* **39**, No. 3, 1589–1598.

Gikas, V. & Sakellariou, M. (2008). Settlement analysis of the Mornos earth dam (Greece): evidence from numerical modeling and geodetic monitoring. *Engng Structs* **30**, No. 11, 3074–3081.

Gurbuz, A. (2011). A new approximation in determination of vertical displacement behavior of a concrete-faced rockfill dam. *Environ. Earth Sci.* **64**, 883–892.

Hanna, A. W., Ambrosii, G. & Mcconnell, A. D. (1986). Investigation of a coarse alluvial foundation for an embankment dam. *Can. Geotech. J.* **23**, No. 2, 203–215.

Hunter, G. J. (2003). *The pre- and post-failure deformation behaviour of soil slopes.* Sydney, Australia: University of New South Wales.

Hunter, G. & Fell, R. (2003). Rockfill modulus and settlement of concrete face fockfill dams. *J. Geotech. Geoenviron. Engng* **129**, No. 10, 909–917.

Icold (International Commission on Large Dams) (2004). *Concrete face rock fill dams concepts for design and construction. Committee on materials for fill dams.* Paris, France: Icold.

Jia, Y. & Chi, S. (2015). Back-analysis of soil parameters of the Malutang II concrete face rockfill dam using parallel mutation particle swarm optimization. *Comput. Geotech.* **65**, 87–96.

Jia, J. S., Xu, Y., Hao, J. T. & Zhang, L. M., (2016). Localizing and quantifying leakage through CFRDs. *J. Geotech. Geoenviron. Engng* **142**, No. 9, 06016007.

Jiang, G. & Cao, K. (1993). Concrete face rockfill dams in China. *Proceedings of international symposium on high earth-rockfill dams*, Beijing, China, pp. 25–37.

Kan, M. E. & Taiebat, H. A. (2016). Application of advanced bounding surface plasticity model in static and seismic analyses of Zipingpu Dam. *Can. Geotech. J.* **53**, No. 3, 455–471.

Karstunen, M. & Yin, Z. Y. (2010). Modelling time-dependent behaviour of Murro test embankment. *Géotechnique* **60**, No. 10, 735–749, https://doi.org/10.1680/geot.8.P.027.

Khalid, S., Singh, B., Nayak, G. C. & Jain, O. P. (1990). Nonlinear analysis of concrete face rockfill dam. *J. Geotech. Engng* **116**, No. 5, 822–837.

Kim, Y. S. & Kim, B. T. (2008). Prediction of relative crest settlement of concrete-faced rockfill dams analyzed using an artificial neural network model. *Comput. Geotech.* **35**, No. 3, 313–322.

Kim, Y. S., Seo, M. W., Lee, C. W. & Kang, G. C. (2014). Deformation characteristics during construction and after impoundment of the CFRD-type Daegok Dam, Korea. *Engng Geol.* **178**, 1–14.

Kyrou, K., Penman, A. D. M. & Artemis, C. C. (2005). The first 30 years of Lefkara Dam. *Proc. Instn Civ. Engrs – Geotech. Engng* **158**, 113–122.

Lawton, F. L. & Lester, M. D. (1964). Settlement of rockfill dams. *Proceedings of the 8th ICOLD congress*, Edinburgh, UK, pp. 599–613.

Li, N. (2007). *Recent technology for high concrete face rockfill dams.* Beijing, China: China Water Conservancy and Hydropower Press.

Li, N. (2011). Performance of high concrete face rockfill dam in China and its inspiration. *Chin. J. Geotech. Engng* **33**, No. 2, 166–173.

Li, M., Wang, X., Xiong, Z. & Chen, H. (2001). CFRD monitoring and its behavior analysis. *J. Yangtze River Sci. Res. Inst.* **18**, No. 1, 45–48.

Li, G., Miao, J. & Mi, Z. (2014). A review of foundation condition and design scheme for seepage prevention system of high CFRD built on deep alluvium deposit. *Hydro-sci. Engng* **4**, No. 4, 1–6.

Lollino, P., Cotecchia, F., Zdravkovic, L. & Potts, D. M. (2005). Numerical analysis and monitoring of Pappadai dam. *Can. Geotech. J.* **42**, No. 6, 1631–1643.

Ma, G., Zhou, W., Ng, T. T., Cheng, Y. G. & Chang, X. L. (2015). Microscopic modeling of the creep behavior of rockfills with a delayed particle breakage model. *Acta Geotechnica* **10**, No. 4, 481–496.

Mahabad, N. M., Imam, R., Javanmardi, Y. & Jalali, H. (2014). Three-dimensional analysis of a concrete-face rockfill dam. *Proc. Instn Civ. Engrs – Geotech. Engng* **167**, No. 4, 323–343.

Downloaded by [UNIV OF ILLINOIS] on [05/02/20]. Copyright © ICE Publishing, all rights reserved.

Mahinroosta, R., Alizadeh, A. & Gatmiri, B., (2015). Simulation of collapse settlement of first filling in a high rockfill dam. *Engng Geol.* **187**, 32–44.

Modares, M. & Quiroz, J. E. (2016). Structural analysis framework for concrete-faced rockfill dams. *Int. J. Geomech.* **16**, No. 1, 04015024.

Özkuzukiran, S., Özkan, M. Y., Özyazicioğlu, M. & Yildiz, G. S. (2006). Settlement behaviour of a concrete faced rock-fill dam. *Geotech. Geol. Engng* **24**, No. 6, 1665–1678.

Pinto, N. L. S. & Marques, F. P. (1998). Estimating the maximum face deflection in CFRDs. *Int. J. Hydropower Dams* **5**, No. 6, 28–31.

Qian, X. X., Yuan, H. N., Li, Q. M. & Zhang, B. Y. (2013). Comparative study on interface elements, thin-layer elements, and contact analysis methods in the analysis of high concrete-faced rockfill dams. *J. Appl. Math.* **2013**, 320890.

Qu, G., Hinchberger, S. D. & Lo, K. Y. (2009). Case studies of three-dimensional effects on the behaviour of test embankments. *Can. Geotech. J.* **46**, No. 11, 1356–1370.

Rice, J. D. & Duncan, J. M. (2010a). Deformation and cracking of seepage barriers in dams due to changes in the pore pressure regime. *J. Geotech. Geoenviron. Engng* **136**, No. 1, 16–25.

Rice, J. D. & Duncan, J. M. (2010b). Findings of case histories on the long-term performance of seepage barriers in dams. *J. Geotech. Geoenviron. Engng* **136**, No. 1, 2–15.

Saboya, F. & Byrne, P. M. (1993). Parameter for stress and deformation analysis of rockfill dams. *Can. Geotech. J.* **30**, No. 4, 690–701.

Seo, M. W., Ha, I. S., Kim, Y. S. & Olson, S. M. (2009). Behavior of concrete-faced rockfill dams during initial impoundment. *J. Geotech. Geoenviron. Engng* **135**, No. 8, 1070–1081.

Sherard, J. L. & Cooke, J. B. (1987). Concrete-face rockfill dam: I. assessment. *J. Geotech. Engng* **113**, No. 10, 1096–1112.

Silvani, C., Désoyer, T. & Bonelli, S. (2009). Discrete modelling of time-dependent rockfill behaviour. *Int. J. Numer. Analyt. Methods Geomech.* **33**, No. 5, 665–685.

Song, H. & Cui, W. (2015). Stop-end method for the panel connection of cut-off walls. *Proc. Instn Civ. Engrs – Geotech. Engng* **168**, No. 5, 457–468.

Sowers, G. F., Williams, R. C. & Wallace, T. S. (1965). Compressibility of broken rock and the settlement of rockfills. *Proceedings of 6th international conference on soil mechanics and foundation engineering*, Toronto, Canada, pp. 561–565.

Su, H., Hu, J. & Wen, Z. (2012). Structure analysis for concrete-faced rockfill dams based on information entropy theory and finite element method. *Int. J. Numer. Analyt. Methods Geomech.* **36**, No. 8, 1041–1055.

Wang, Y. S. & Liu, S. H. (2005). Treatment for a fully weathered rock dam foundation. *Engng Geol.* **77**, No. 1–2, 115–126.

Wang, Z., Liu, S., Vallejo, L. & Wang, L. (2014). Numerical analysis of the causes of face slab cracks in Gongboxia rockfill dam. *Engng Geol.* **181**, 224–232.

Wei, Z., Xiaolin, C., Chuangbing, Z. & Xinghong, L. (2010). Creep analysis of high concrete-faced rockfill dam. *Int. J. Numer. Methods Biomed. Engng* **26**, No. 11, 1477–1492.

Wen, L., Qin, Y., Chai, J., Li, Y., Wang, X. & Xu, Z. (2015). Behaviour of concrete-face rockfill dam on sand and gravel foundation. *Proc. Instn Civ. Engrs – Geotech. Engng* **168**, No. 5, 439–456.

Wen, L., Chai, J., Xu, Z., Qin, Y. & Li, Y. (2017). Monitoring and numerical analysis of behaviour of Miaojiaba concrete-face rockfill dam built on river gravel foundation in China. *Comput. Geotech.* **85**, 230–248.

Won, M. S. & Kim, Y. S. (2008). A case study on the post-construction deformation of concrete face rockfill dams. *Can. Geotech. J.* **45**, No. 6, 845–852.

Xiao, Y., Liu, H., Chen, Y., Jiang, J. & Zhang, W. (2015). State-dependent constitutive model for rockfill materials. *Int. J. Geomech.* **15**, No. 5, 04014075.

Xing, H. F., Gong, X. N., Zhou, X. G. & Fu, H. F. (2006). Construction of concrete-faced rockfill dams with weak rocks. *J. Geotech. Geoenviron. Engng* **132**, No. 6, 778–785.

Xu, Z., Hou, Y. J. & Han, L. (2006). Centrifuge modeling of concrete faceed rockfill dam built on deep alluvium. In *Physical modelling in geotechnics* (eds C. W. W. Ng, Y. H. Wang and L. M. Zhang), pp. 435–440. London, UK: Taylor & Francis Group.

Xu, B., Zou, D., Kong, X., Hu, Z. & Zhou, Y. (2015). Dynamic damage evaluation on the slabs of the concrete faced rockfill dam with the plastic-damage model. *Comput. Geotech.* **65**, 258–265.

Zhang, G. & Zhang, J. M. (2009). Numerical modeling of soil–structure interface of a concrete-faced rockfill dam. *Comput. Geotech.* **36**, No. 5, 762–772.

Zhang, G. & Zhang, J. M. (2011). Modeling of low-cement extruded curb of concrete-faced rockfill dam. *Can. Geotech. J.* **48**, No. 1, 89–97.

Zhang, B., Wang, J. G. & Shi, R. (2004). Time-dependent deformation in high concrete-faced rockfill dam and separation between concrete face slab and cushion layer. *Comput. Geotech.* **31**, No. 7, 559–573.

Zhang, G., Zhang, J. M. & Yu, Y. (2007). Modeling of gravelly soil with multiple lithologic components and its application. *Soils Found.* **47**, No. 4, 799–810.

Zheng, D., Cheng, L., Bao, T. & Lv, B. (2013). Integrated parameter inversion analysis method of a CFRD based on multi-output support vector machines and the clonal selection algorithm. *Comput. Geotech.* **47**, 68–77.

Zhou, W., Hua, J., Chang, X. & Zhou, C. (2011). Settlement analysis of the Shuibuya concrete-face rockfill dam. *Comput. Geotech.* **38**, No. 2, 269–280.

Downloaded by [UNIV OF ILLINOIS] on [05/02/20]. Copyright © ICE Publishing, all rights reserved.